Measuring the Climate Risk Spillover through Financial Markets

Runfeng Yang[*], Juan-Angel Jiménez-Martin[†] and Massimiliano Caporin[‡]

Abstract

Climate risk, the risk generated during the process of climate change, now becomes a global issue that affects multiple regions and countries. As a result, climate risk in one region could transfer to another region. In this paper, we study the climate risk spillover through the channel of financial markets. We propose a new method to capture the climate risk. Then, we study the climate risk spillover through testing pair-wise Granger Causality in risk and through constructing the connectedness network in six major markets. We find that Europe and the US are the main climate risk transmitters, and China and Japan are the main receivers of the climate risk. It takes around three weeks for climate risk to be fairly transmitted and around 30% of local climate risk shocks comes from outside. When there are large-scale climate events, the US and Europe are the main sources of risk transmission. A higher climate sentiment leads to a higher level of risk transmission. We also find that when the economic activities are low, the level of climate risk transmission is also low.

Keywords: Climate Change, Long-short Portfolio, Climate Risk, Granger Causality, Connectedness Network, Carbon Emission

[*]Instituto Complutense de Análisis Económico (ICAE), Universidad Complutense de Madrid, author email: runfengy@ucm.es

[†]Instituto Complutense de Análisis Económico (ICAE), Universidad Complutense de Madrid, author email: juanangel@ccee.ucm.es

[‡]Department of Statistical Sciences, University of Padova, author email: massimiliano.caporin@unipd.it

Contents

1 Introduction

Climate risk, or the climate change risk, can be categorized into two types: physical risk and transition risk. The physical risk is the direct damage caused by the climate change, for example, the damage to the local economy due to a strong hurricane; and the transition risk is the impact on companies due to a possible transition to a green economy (e.g., government carbon taxes). One crucial property of the climate risk is that it can "transmit" across boarders. That is, through socioeconomic connections among countries, local climate change events could have impacts to other regions. And such impact is not trivial. A report studying the climate change impact for UK reached a conclusion that cross-border climate change impacts on trade, investment and food systems are larger than domestic impacts (PwC, 2013). In addition, national assessments of cross-border climate change impacts have been made in a number of countries within the EU and also for the whole EU region.[1] In the most recent Intergovernmental Panel on Climate Change (IPCC) report, the transmission nature of climate risk has been further emphasized.[2]

If climate risk can transmit across borders and have considerable impacts, then an important part of measuring the climate risk impact is to measure how and to which extent it could transfer across borders. The "transmit nature" of climate risk also poses additional challenges for regulators to properly evaluate the impact of climate change on local economy. As for the financial markets, the spillover of climate risk from other regions also means another source of risk. That is, for banks and investors whose assets have high exposure to climate risk, they not only have to evaluate domestic climate impacts but also foreign impacts in order to manage the climate risk. For this purpose, various recent studies try to provide a discussion how we we should measure climate risk spillovers (Li et al., 2021, Carter et al., 2021, West et al., 2021, Benzie et al., 2019 and Challinor et al., 2018). Benzie et al. (2019) summarize four possible pathways through which climate risk can spillover across borders: Finance, People, Trade, Biophysical.[3] However, none of these studies are able to provide a method to quantify the climate risk spillover, that is, to measure extent to which the climate risk can transmit across borders.

One possible difficulty is that the climate risk is hard to measure because of the complex interactions and uncertainties in the Earth and human systems (Diaz and Moore, 2017). However, recent empirical studies find that climate risk is now being priced and realized in the financial market (Giglio et al., 2021 and Engle et al., 2020), which gives us some hinds on how to capture the climate risk. The theory is that, long-run physical or transition risk is gradually realized over time as climate events, and such climate events is captured by two indicators. The first indicator is climate change news – climate events are reported in climate change news. The other indicator is

[1] For example, Netherlands, Germany, Norway, Switzerland, Finland, etc., as summrized by Benzie et al. (2019) and Carter et al. (2021). West et al. (2021) study the cross-border climate change impact for the whole Europe

[2] In the report, they conclude that the observed climate risk are "complex risks result from multiple climate hazards occurring concurrently, and from multiple risks interacting, compounding overall risk and resulting in risks transmitting through interconnected systems and across regions".

[3] The biophysical pathway can be cross-border ecosystems (e.g. floods or droughts upstream in a river basin); the trade pathway are consisted of international markets; the finance pathway means the flow of public and private capital; the people pathway means the movement of people across borders.

similar: while climate events is reflected as the arrival of climate news, it can also be reflected in the investor's climate sentiment. The climate sentiment is a concept similar to market sentiment, and it measures the investors optimistic or pessimistic beliefs about climate change that are not based on the facts at hand (Santi, 2022 and Baker and Wurgler, 2006). Then, changes in the two indicators are captured in the financial market. For example, investors who receive information from climate change news will update their beliefs; then, they will adjust their holdings, which would then cause asset prices to move. In sum, long-term climate risks are realized as climate events, which then are reflected in climate news or changes of climate sentiments, and are finally reflected the asset price.

If the climate risk is being priced and realized in the financial market, then we can form a portfolio that follows the climate risk (as done by Engle et al., 2020). To form such portfolios, we can either construct a portfolio that follows the climate news arrivals, or that captures the changes in the climate sentiment. On way documented by the literature is to use the return difference between portfolios with high environmental performance and low environmental performance. For example, Pastor et al. (2021) show that the return difference between green (with higher environmental performance) and brown stocks interacts with changing investor environmental concern. Engle et al. (2020) show that the return difference between green and brown stocks explains large part of the climate changes news innovation. If a portfolio follows closely to changes in the climate risk, then changes in the portfolio return can serve as a proxy for the climate risk. And once we get the proxy for the climate risk, we can study the climate risk spillover by studying how such proxy of climate risk in different markets interacts with each other.

Leaning on previous findings, this paper studies the climate risk spillover in a quantitative manner: to measure how much and to which extent the climate risk can transmit across borders through the financial markets. For this purpose, we first construct the climate risk hedge portfolio, a portfolio that is supposed to follow the climate risk, the return difference between portfolios with high environmental performance and low environmental performance. Specifically, we use the return difference high-emission and low-emission companies and calculate it using the two-sort method of Fama and French (1993). We then proxy the climate risk as changes in such long-short portfolio. Once we have the proxy for climate risk, we measure the climate spillover by studying how such proxy in different markets interacts with each other.

We study the level of interaction for two scenarios: when there are extreme positive climate shocks and extreme negative shocks. For this purpose, we first check the pair-wise Granger causality in risk, propose by Hong et al. (2009), between two markets. We further construct the connectedness network at 5% and 95% quantiles to study the level of the climate risk spillover among financial markets, for which we apply the Quantile VAR model (Chavleishviliy and Manganelli, 2021 and Montes-Rojas, 2019), the VAR model at different quantiles, and the connectedness table proposed by Diebold and Yilmaz (2014). We study six major markets globally: the United States, China (including Hong Kong), Europe (including UK), Canada, Australia and Japan. Though these methods, we try to answer the following question: to which extent an observed local climate risk shock is consisted of foreign climate risk shock?

In line with Bolton and Kacperczyk (2022), we find that the climate risk is being priced in the six markets, with each market having different levels of prices. Also, the trends are similar among different markets: when there are global-level climate events such as the signing of Paris Agreement, every market responds similarly. After getting the proxy, we study the pair-wise risk spillover among the six markets. We study two scenarios: when there are extreme positive climate risk shocks and extreme negative climate risk shocks. We find that the climate risk spillover among countries depends on the type of climate risk shock (positive or negative) as well as the country. In general, we find that Japan is the most segregated market and the US is the market that receives and gives the highest level the climate risk. The level of climate risk spillover is the highest around the event of Paris Agreement and the outbreak of COVID.

We then put the six market in a network to study the level of climate risk spillover. We find that it takes around three weeks for climate risk to be fairly transmitted. On average, around 30% of the local climate risk comes from outside within five weeks. The level of spillover is higher for negative climate risk shocks than for positive climate risk shocks. Europe, US and Canada are the main climate risk transmitters, and China and Japan are the main receivers of the climate risk. However, the role could change across time. For example, the US changed from net risk transmitters (during the Paris Agreement period) to net receivers (after the period). It is thus important to understand the cause of climate risk shock and the characteristics of corresponding markets before analyzing the climate risk spillover.

We also study the determinants of the climate risk spillover. When financial markets are more connected, climate risk can transfer more easily. A higher level of trading activities will facilitate the transmission of climate risk, especially during the pre-COVID period. In addition, we show that a higher global climate sentiment means that the level of risk spillover is also higher.

The contribution of our paper is three-fold. First, we provide a new method to quantify and proxy the climate risk in the market. The method can be used by investors to calculate the climate risk exposure of their portfolios. For regulators, such proxy of climate risk could be used in economic models to formulate climate-change-related policies. Second, we quantify the risk spillover by building a connectedness network, which can offer a reference to future researches on how to measure the climate risk spillover. Third, we provide empirical evidence to the current literature on how and to which extent the climate risk is transmitted through financial markets globally.

The paper is organized as follows. We first provide a discussion in Section 2 to show how we capture the climate risk and how we measure the risk spillover. We then describe in Section 3 the data we use. In Section 4 we present the discussion of the climate risk in different markets. Section 5 and 6 shows how and to which extent the climate risk is transmitted across markets. We deepen our discussion in Section 7 by investigating the determinants of the climate risk spillover. We give the conclusion in Section 8.

2 Methodology

2.1 Capturing Climate Risk

Long-term climate risks are realized as climate events and these climate events are reported in climate news, news whose theme is about climate change (disasters, regulations, etc.). Investors who see the news may change their climate sentiments (i.e., the investor's optimistic or pessimistic beliefs about climate change). Then, either the arrival of climate news or changes in climate sentiments are evidenced in the literature to be reflected as changes in asset prices in the financial market. Thus, a portfolio/asset whose return follows the arrival of climate news or changes in climate sentiments can be used as a proxy for climate risk. In recent empirical literature, one type of portfolio is found to be associated with both climate news and climate sentiments: the return difference between companies with high environmental performance and low environmental performance, defined as,

$$R_t^E \equiv R_t^{High\,E} - R_t^{Low\,E}, \tag{2.1}$$

where $R_t^{High\,E}$ is the return of a portfolio that consists of companies with high environmental score (high-E) and $R_t^{High\,E}$ is the return of a portfolio that consists of companies with low environmental score (low-E).[4] Engle et al. (2020) run a regression between climate change news indices and R_t^E.[5] They find that R_t^E can explain a large part of the news index. Similarly, Pastor et al. (2021) run a regression between R_t^E and an index that measures the climate sentiment, and they show that R_t^E can be explained by the climate sentiment. In a similar vein, Choi et al. (2020) show that when the local temperature is abnormally high, people revise their beliefs about climate change and in the financial market, stocks of high-emission firms (and thus low environmental performance) under-perform firms with low emissions. Santi (2022) shows that stocks of high-emission firms under-perform low-emission ones when investor climate sentiment increases.

We will apply similar long-short portfolio in our paper to capture the climate risk. In constructing R_t^E, the environmental score is used to group companies into high-E and low-E (to calculate $R_t^{High\,E}$ and $R_t^{Low\,E}$), which can be problematic. One issue is that while there are many data providers in the market offering the rating, the correlation among them is quite low, and thus the score suffers from measurement error (Berg et al., 2021). As a result, a change of data provider could possibly result in a change of the R_t^E. Thus, instead of using the environmental score to construct the R_t^E, we use the carbon emission of each company, which is more objective than the environmental score. Although the carbon emission can not represent the whole picture of a company's environmental performance that affects the climate change, the main driver of climate

[4]The environmental score is a credit-rating-like score that measures the environmental performance of a company (i.e., if a company's business model is environmental friendly), usually based on a matrix of indicators. A high Environmental score means high environmental performance, for which we call companies with high environmental scores high-E companies.

[5]The climate change news index, for example the WSJ Climate Change News Index, is an keyword-based news index that measures the amount of climate change news in a given time. A higher index value usually means the during the period there are many reports about the climate change, indicating the happening of climate change events.

change is the greenhouse effect due to greenhouse gas emission, and carbon emission is the major greenhouse gas.[6] The high level of CO2 concentration in the atmosphere is believed to be largely responsible for human-induced climatic change (Rehan and Nehdi, 2005).

In concrete, we capture the climate risk by following steps. We first construct the long-short portfolio as:

$$R_t^C \equiv R_t^{Low\,Ems} - R_t^{High\,Ems}, \tag{2.2}$$

where $R_t^{Low\,Ems}$ is the return of low-emission portfolios and $R_t^{High\,Ems}$ is the return of high-emission portfolios.

Because climate events are reflected as changes in the long-short portfolio, we then estimate the AR (1) process for the return of the long-short portfolio:

$$R_t^C = \alpha + \beta R_{t-1}^C + u_t. \tag{2.3}$$

Finally, we capture the climate risk as the innovation (u_t) of the above AR(1) model as:

$$CRisk_t \equiv \hat{u}_t = R_t^C - \hat{\alpha} - \hat{\beta} R_{t-1}^C. \tag{2.4}$$

We use the innovation of the AR(1) process to emphasis the "unexpected" part of the changes, because investors update their beliefs only when the information is unexpected. In Eq. (2.2), we try to capture the information of climate sentiment/climate change news using the return difference between two portfolios with different levels of carbon emission. Then, we use the unexpected change of the long-short portfolio as a representation of climate risk. We provide in Appendix B a detailed description of the process we use to construct the portfolio, which follows closely the two-sort process of Fama and French (1993).

It is worth discussing the interpretation of $CRisk_t$ before moving on. Climate events (extreme weather, climate-change-related regulations, etc.) are one type of shocks, and such shocks may generate changes in the climate sentiment or are reflected in climate change news, which would then cause investors to update their climate change beliefs, and then a change in the return of the long-short portfolio. In other words, climate-related events could trigger investor actions and finally changes the value of the portfolio. In short, $CRisk_t$ is the realization of climate change shocks in the financial market.

$CRisk_t$ should be close to zero in normal times. Then, when climate change events happen, we can observe changes in the the long-short portfolio (be it positive or negative). When there are positive changes ($CRisk_t > 0$), it means that there are positive shocks from climate events that pushes an increase in the demand for low-emission companies, for example, the signing of Paris

[6] https://ec.europa.eu/clima/climate-change/causes-climate-change_en

Agreement or a large-scale extreme weather. When there are negative changes ($CRisk_t < 0$), it means a shock that causes high-emission companies to outperform low-emission one, which could be the result of a reduction of carbon tax or a relief of global warming.

After getting the numerical measure of $CRisk_t$ as a proxy for the climate risk, we study the climate risk spillover by looking at two situations: when $CRisk_t$ is extremely high (when $CRisk_t$ is at its 95% quantile) and extremely low (when $CRisk_t$ is at its 5% quantile). We study the extreme changes of the long-short portfolio for two reasons. First, small changes of the portfolio R_t^C could be due to normal market fluctuations but not necessarily climate events. Second, from a risk management perspective, what worries investors and regulators most is the climate risk that may cause huge fluctuations in the market and in their asset value.

2.2 Granger Causality in Risk

We first apply the Greager causality analysis to study the relationship of $CRisk_t$ in different markets. To study the relationship at different quantiles, we apply the test of Granger causality in risk proposed by Hong et al. (2009), which is an extension of the Granger causality proposed by Granger (1969). The interpretation is that, if two markets have Granger causality in risk relationship, then the occurrence of a large risk in one market can help predict the occurrence of the large risk in another market. Put it in our case: if the climate risk ($CRisk_t$) of the US Granger-causes the climate risk in China at 95%, it means that when there are large shocks from climate events in the US, such that $CRisk_t$ in the US becomes very large (changes to its 95% quantile), it contributes to the future case where $CRisk_t$ in China becomes very large (change to 95%). Since the extreme change of the long-short portfolio can have two directions: upside and downside, we consider two types of Granger causality in risk: down-to-down and up-to-up. We don't consider in this paper the situation of down-to-up and up-to-down because international evidence show that investors in different markets react similarly to the climate risk (Bolton and Kacperczyk, 2022). Thus, it is less likely that a negative extreme shock in one market would turn into a positive extreme shock in other market.

Following Hong et al. (2009) and the discussion in Du and He (2015), we first define the quantile of two time series $\{Y_{i,t}\}_{t=1}^{T}, i = 1, 2$ series as

$$Prob\left[Y_{i,t} \leq q_{i,t}^{\tau} \mid \mathcal{F}_{t-1}\right] = \tau,$$

where $\mathcal{F}_{t-1}$ denotes the information set until $t-1$ and τ is the probability level and $q_{i,t}^{\tau}$ is the conditional quantile at time t for series $Y_{i,t}$. In our case, $\tau = 5\%$. Then we define the two types of risk hit series $\{Z_{i,t}\}_{t=1}^{T}, i = 1, 2$ as

$$Z_{i,t}^{\text{Down}} = \begin{cases} 1 & \text{if } Y_{i,t} < q_{i,t}^{\tau} \\ 0 & \text{else} \end{cases},$$

$$Z_{i,t}^{\text{Up}} = \begin{cases} 1 & \text{if } Y_{i,t} > q_{i,t}^{1-\tau} \\ 0 & \text{else} \end{cases}.$$

Then, the null and alternative hypotheses are (taking the down-to-down for example)

$$\mathbb{H}_0 : \mathbb{E}\left[Z_{1,t}^{\text{Down}} \mid I_{1,t-1}^{\text{Down}}\right] = \mathbb{E}\left[Z_{1,t}^{\text{Down}} \mid I_{1,t-1}^{\text{Down}}, I_{2,t-1}^{\text{Down}}\right], \tag{2.5}$$

$$\mathbb{H}_1 : \mathbb{E}\left[Z_{1,t}^{\text{Down}} \mid I_{1,t-1}^{\text{Down}}\right] \neq \mathbb{E}\left[Z_{1,t}^{\text{Down}} \mid I_{1,t-1}^{\text{Down}}, I_{2,t-1}^{\text{Down}}\right], \tag{2.6}$$

where $I_{i,t-1}^{\text{Down}}, i = 1, 2$ is the information set for series $Y_{i,t}$ at time $t-1$. Therefore, if the null hypothesis is rejected and we accept the alternative, it means that when Y_2 changes below the quantile level $q_{2,t}^{\alpha}$, it has significant impact to the probability of a future occurrence of a hit in $Y_{1,t}$, and we say that $Y_{2,t}$ Granger-causes $Y_{1,t}$ in the quantile α.

To calculate test statistics, we calculate the sample cross-correlation between the two hit series$\{Z_{1,t}\}_{t=1}^{T}$ and$\{Z_{2,t}\}_{t=1}^{T}$ as:

$$\hat{\rho}(j) = \frac{\hat{C}(j)}{\hat{S}_1 \hat{S}_2}$$

where $\hat{S}_i = \sqrt{\hat{\tau}_i(1-\hat{\tau}_i)}$ (the hit series $\hat{Z}_{i,t}$ follows an i.i.d. Bernoulli $(\hat{\tau}_i)$ distribution, with $\hat{\tau}_i = \frac{1}{T}\sum_{t=1}^{T} \hat{Z}_{i,t}$), j is the lag order, with $j = \{1, 2, ..., T-1\}$ and sample cross-covariance $\hat{C}(j)$ is calculated as:

$$\hat{C}(j) = \frac{1}{T} \sum_{t=1+j}^{T} \left(\hat{Z}_{1,t} - \hat{\tau}_1\right)\left(\hat{Z}_{2,t-j} - \hat{\tau}_2\right).$$

Thus, the test statistic of one-way Granger causality in risk from $Y_{2,t}$ to $Y_{1,t}$ is

$$Q_1(M) = \frac{T\sum_{j=1}^{T-1} k\left(\frac{j}{M}\right)^2 \hat{\rho}(j)^2 - C_{1,T}(M)}{D_{1,T}(M)^{1/2}} \xrightarrow{D} N(0,1), \tag{2.7}$$

with

$$\begin{cases} C_{1,T}(M) \equiv \sum_{j=1}^{T-1}(1-\frac{j}{T})k^2(\frac{j}{M}) \\ D_{1,T}(M) \equiv 2\sum_{j=1}^{T-1}(1-\frac{j}{T})\left(1-\frac{(j+1)}{T}\right)k^4(\frac{j}{M}) \end{cases},$$

where M is the maximum lag order that we consider for the analysis of risk spillover, with $M = cT^v, c > 0, 0 < v < \frac{1}{2}$. If $M = 5$, it means we are testing if the risk spillover from $Y_{2,t}$ to $Y_{1,t}$ is statistically significant within five lags. Since we do not know at which lag the climate risk will transfer across markets, we will discuss in the empirical analysis part the Granger causality in risk under different lag orders.

$k(x)$ is a suitable kernel function, which in our case is the Daniell kernel $k(x) = \frac{\sin(\pi x)}{\pi x}$, because Hong et al. (2009) show that Daniell kernel maximizes the asymptotic power of $Q_1(M)$. If $Q_1(M)$ is larger than some critical value given a certain confidence level (for example, 1.65 at 95%, one-sided), then we say that $Y_{2,t}$ Granger-causes $Y_{1,t}$ at the given quantile.

To estimate the hit series $(\hat{Z}_{i,t})$, we need to estimate the conditional quantile series $q^{\tau}_{i,t}$. We use the method proposed by Engle and Manganelli (2004) called *conditional auto-regressive value at risk (CAViaR)*, where the quantile is estimated by directly modeling the distribution of the quantile without distributional assumptions. We are going to use the Symmetric CAViaR, with the setting as:

$$q^{\tau}_t = \beta_0 + \beta_1 q^{\tau}_{t-1} + \beta_2 \mid CRisk_{t-1} \mid,$$

where the initial value q^{τ}_0 is given by the historical quantile of the whole sample period; $CRisk_t$ is the climate risk series in the previous section.

2.3 Risk Spillover Measure

The Granger causality in risk analysis only shows if climate risk transmits across two markets. However, with only the Granger causality in risk analysis, it is hard to show the level (how much) of risk spillover. To do so, we apply the framework of quantile vector autoregressive (Quantile VAR) model. The Quantile VAR model is similar to the VAR model except that every equation in the system is quantile regression. The model can be used to evaluate the interaction of quantiles of endogenous variables in the system. Then, based on the model, we conduct the simulation-based generalized variance decomposition proposed by Lanne and Nyberg (2016) and finally construct the risk spillover table based on the connectedness network of Diebold and Yilmaz (2014). The connectedness network should tell the the level of climate risk spillover.

2.3.1 Quantile VAR Model (QVAR)

We refer to the discussion in Su (2020) and Chen et al. (2022) to apply the quantile VAR model. The basic element of the QVAR model is quntile regression. The quantile regression explains the τth quantile a time series (Y_t) given the vector of explanatory variables X_t :

$$F^{-1}(\tau, Y_t|covariates) = X_t\beta(\tau), \tag{2.8}$$

where $F^{-1}(Y_t)$ is the probability distribution function of the random variable. $\beta(\tau)$ is estimated conducting the following minimization.

$$\beta(\tau) = \underset{\beta(\tau)}{arg\min} \sum_{t=1}^{T} (\tau - 1_{\{Y_t < X_t\beta(\tau)\}}) \left| Y_t - X_t\beta(\tau) \right|.$$

The M-order quantile VAR process of n-variable is as follows:

$$Y_t = c(\tau) + \sum_{i=1}^{M} B_i(\tau) Y_{t-i} + \epsilon_t(\tau), \quad t = 1, ..., T, \tag{2.9}$$

with

$$Q(\tau, Y_t) = c(\tau) + \sum_{i=1}^{M} B_i(\tau) Y_{t-i},$$

where Y_t is the K-vector of endogenous time series; τ is the level of quantile and in our case, $\tau = 5\%\&95\%$; K is the number of variables. $c(\tau)$ is the K-vector of intercepts at quantile τ. $B_i(\tau)$ for $i = 1, ..., M$ is the lagged coefficients for quantile τ. Each equation in the quantile VAR system is estimated under quantile regression in Eq.(2.8) (i.e., $B_i(\tau)$ comes from the quantile regression estimation). $\epsilon_t(\tau)$ is the vector of residual terms, with $Q(\tau, \epsilon_t(\tau) \mid Y_{t-1}, ..., Y_{t-M}) = 0$. The stationary condition of the QVAR model is similar to the VAR in the mean.[7]

2.3.2 Quantile General Forecast Error Variance Decomposition (QGFEVD)

Based on the QVAR model, we apply a the Quantile GFEVD based on the GFEVD proposed by Lanne and Nyberg (2016):

$$\lambda_{ij}(H) = \frac{\sum_{h=0}^{H-1} \left[QGI_Y(H, \epsilon^*_{j,t}(\tau), \mathcal{F}_{t-1})_i \right]^2}{\sum_{h=0}^{H-1} \sum_{j=1}^{n} \left[QGI_Y(H, \epsilon^*_{j,t}(\tau), \mathcal{F}_{t-1})_i \right]^2}, \tag{2.10}$$

where $QGI_Y(H, \epsilon^*_{j,t}(\tau), \mathcal{F}_{t-1})$ is the Quantile Impulse Response Function (QIRF), defined as:

$$QGI_Y(H, \epsilon^*_{j,t}(\tau), \mathcal{F}_{t-1}) \equiv Q\left(\tau, Y_{t+H} \mid \epsilon^*_{j,t}(\tau) = \epsilon_{j,t}(\tau) + \delta_j, \mathcal{F}_{t-1}\right) - Q\left(\tau, Y_{t+H} \mid \mathcal{F}_{t-1}\right). \tag{2.11}$$

$Q(\tau, Y_{t+H} \mid \epsilon^*_{j,t}(\tau) = \epsilon_{j,t}(\tau) + \delta_j, \mathcal{F}_{t-1})$ is the conditional quantile of Y_{t+H} given a shock δ_j at time t. $Q(\tau, Y_{t+H} \mid \mathcal{F}_{t-1})$ is the conditional quantile without the shock. Therefore, the above definition of QIRF means that, given the K-variable QVAR system of (2.9), we give a shock to the residual of variable j ($\epsilon_{j,t}(\tau)$) at time t and check how the quantile of Y_t changes H periods after.[8] $QGI_Y(H, \delta_j, \mathcal{F}_{t-1})$ is thus a $(K \times 1)$ vector that shows the response of the K-variable QVAR system to a variable specific shock of j in H periods. Accordingly, $QGI_Y(H, \delta_j, \mathcal{F}_{t-1})_i$ (with subscript i) is the ith element of the vector, and measures the response of variable i to the shock j in H periods.

In addition, if we choose the shock (δ_j) from the history of quantile residuals $\epsilon(\tau)$, then a shock at time t to Y_t means that Y_t changes to its τth quantile (i.e.,$\delta_j = -\epsilon_m(\tau) \Rightarrow Y^*_{j,t} = c(\tau) + \sum_{i=1}^{M} B_i(\tau) Y_{t-i} + \epsilon_t(\tau) - \epsilon_m(\tau) = Y_{j,t} - \epsilon_m(\tau) = Q_m(\tau, Y_{j,t})$). Note that $\epsilon(\tau)$ is usually positive for $\tau < 50\%$ and negative for $\tau > 50\%$. Then, the QIRF has an economic interpretation in our case:

[7] See proposition 1 of Chavleishviliy and Manganelli (2021).

[8] The definition of QIRF is still under discussion in the literature, see, for example, Chavleishviliy and Manganelli (2021), Montes-Rojas (2019), Han et al. (2019) and White et al. (2015). The key here is to define it properly to answer our research question. The definition in our paper refers partly to Montes-Rojas (2019).

at time t, when there are large shocks from climate events, such that climate risk in the market j become very large/small (changes to its τth quantile), how and to which extent it could contribute to the extreme climate risk of other markets H periods after. Therefore, QIRF provides additional information to the Granger causality test in risk by showing how much the climate risk is spilled over among different markets.

Given the definition of QIRF, the numerator of QGFEVD in Eq. (2.10) measures the aggregate cumulative (from $h = 0$ to $H - 1$) response of variable i to shock j, and the denominator is the cumulative response of variable i to all shocks (i.e., we give shock to every variable). Therefore, $\lambda_{ij}(H)$ shows the percentage response of variable i to shock j and by construction, $\Sigma_{j=1}^{n}\lambda_{ij}(H) = 1$.

One thing worth mentioning is that the quantile residual ($\epsilon_t(\tau)$) is different from the error in the mean (ϵ_t). In Koop et al. (1996) and Pesaran and Shin (1998)'s work, the generalized impulse response function is based on the the error in the mean (ϵ_t):

$$\begin{aligned} GI_Y(H, \delta_j, \mathcal{F}_{t-1}) &= E(Y_{t+H} \mid \epsilon_{jt} = \delta_j, \mathcal{F}_{t-1}) - E(Y_{t+H} \mid \mathcal{F}_{t-1}) \\ &= A_H E(\epsilon_t \mid \epsilon_{jt} = \delta_j) = A_H \Sigma e_j \sigma_{jj}^{-1} \delta_j \end{aligned},$$

where A_H is the MA representation coefficient of a VAR model; ϵ_t is assumed to follow multi-variant normal distribution, such that $E(\epsilon_t \mid \epsilon_{jt} = \delta_j)$ has an analytical solution: $E(\epsilon_t \mid \epsilon_{jt} = \delta_j) = \Sigma e_j \sigma_{jj}^{-1} \delta_j$. In comparison, the only restriction put on the $\epsilon_t(\tau)$ is $Q_\tau(\epsilon_t(\tau) \mid Y_{t-1}, ..., Y_{t-p}) = 0$. Therefore, unless we make further distributional assumptions about the quantile error $\epsilon_t(\tau)$, we may not be able to get an explicit function of $QGI_Y(H, \epsilon_{j,t}^*(\tau), \mathcal{F}_{t-1})$, which means that a simulation-based method is needed. We provide in Appendix C on how we use simulation-based method to calculate the QIRF.

After getting the forecast error decomposition, we apply the connectedness framework of Diebold and Yilmaz (2014) and calculate directional spillover form variable j to variable i as:

$$\Sigma_{j=1}^{n}\widetilde{\lambda}_{ij}(H), j \neq i.$$

And the directional spillover form variables i to other variable j is measured as:

$$\Sigma_{i=1}^{n}\widetilde{\lambda}_{ij}(H), i \neq j.$$

Given these directional spillover, net volatility spillovers from market i to all markets j can be calculated as the difference between gross volatility shocks transmitted to and gross volatility shocks received from all other markets:

$$S(H) = \Sigma_{i=1}^{n}\widetilde{\lambda}_{ij}(H) - \Sigma_{j=1}^{n}\widetilde{\lambda}_{ij}(H), i \neq j. \tag{2.12}$$

Finally, we check the total spillover index as:

$$TS = \frac{1}{n}\sum_{i,j=1}^{n}\widetilde{\lambda}_{ij}(H), i \neq j. \tag{2.13}$$

3 Data

3.1 Company Data

Six major markets are included in our sample: the United States, China (including Hong Kong), Europe (including UK), Canada, Australia and Japan. The weekly return for each company will be used and is calculated in a logarithm manner as $R_{i,t} = Ln(\frac{P_{i,t}}{P_{i,t-1}})$ for each company i and time t in each market. In total, we have 443 weekly return observations from 2013/01/07 to 2021/06/28. We do not include the time period in earlier years because there were not many companies disclosing their sustainability information. In addition, the climate sentiment is a phenomenon that appear in only recent years (Giglio et al., 2021). In the US, we have 1920 companies in the sample; in China, we have 464 companies; Japan, 420 companies; Canada, 293 companies; Australia, 310 companies and for Europe, we have 1310 companies.

3.2 Carbon Emission

The Ekion Datastream Database will be used in our analysis. We study the global market and download the month-end carbon emission measure for companies with available data from 2012/12 to 2021/05 (103 months of data in total). Appendix A shows the data and the corresponding code we use in Eikon's database.

In concrete, we use the "Estimated CO2 Equivalents Emission Total", which shows the total CO2 and CO2 equivalents emission in tonnes in one year at a company-level, which include both direct (scope 1) and indirect (scope 2) emissions. The data comes from either company's self-disclosure in the annual report, or from the carbon emission model developed by Eikon, which follows the green house gas emission protocol.[9] To account for the size effect, we also download the month-end value of market value for each company, and we calculate the emission to market value (MV) as:

$$C_{m,i} = \frac{CO2_{m,i}}{MV_{m,i}}, \tag{3.1}$$

where $CO2_{m,i}$ is the month-end value of carbon emission of that year for company i. Note that $CO2_{m,i}$ is updated annually but not necessarily at the beginning of each year (due to different fiscal years of each company), and for this reason we download the month-end value of the carbon emission for each company. The data will be used in calculating the long-short portfolio.

4 Climate Risk in Different Markets

4.1 Climate Risk Statistics

Table 1 shows the statistics of climate risk time series for each market. From Panel A, we can see that Canada has the highest level of standard deviations, followed by Australia. Europe and the

[9]https://www.refinitiv.com/content/dam/marketing/en_us/documents/fact-sheets/esg-carbon-data-estimate-models-fact-sheet.pdf

US have the lowest standard deviation. Panel B shows the correlation among different climate risk time series. The correlation among the US, Europe and Canada is high, indicating that there could be some common factors that drive the co-movement among these markets.

[Insert Table 1 Here]

Figure 1 shows the graphs of the climate risk time series. We observe that climate risk in different markets have similar trends over the years: when major climate events happen, we see huge positive/negative values of the climate risk series, which implies that the climate risk series could reflect the climate change news. In normal times when there are no major climate events, for example form mid-2017 to mid-2019, the climate risk series have small fluctuations. This observation supports our choice of studying the climate risk spillover through extreme values of $CRisk_{i,t}$ (5% and 95%) – major climate events are closely associated with large values of $CRisk_{i,t}$.

Apart from having similar trends, there are two major differences among climate risk series in different markets. The first is that, upon the arrival of a global climate change event, different markets respond with different strengths. For example, after the 2014 UN climate summit, we observe a sharp positive value in Canada (Panel B of Figure 1) but a moderate positive value in EU and US; and the positive value observed in China and Japan are quite small. One possible explanation is that investors in different markets may have different criteria/tastes for climate change, such that the same climate change events could trigger different levels of reactions. The second difference is that during periods where there are no global-wide events (2018 – 2019), the climate risk in different markets are different. This could be due to that climate events in different markets are different.

An interesting observation is that, when the COVID-19 crisis (an event that is not related to climate change) happened, there were also huge positive values observed (e.g., Panel B, Canada, the green line). This could be explained by that during the crisis, investor's preference over green assets strengthened and there are sudden fund inflow into low-emission companies. Dong et al. (2019) explain such phenomenon as "flight to quality" effect: during crisis periods, investors change from low sustainability performance stocks to high sustainability performance stocks. This points to a fact: while investor's climate sentiment could be an indicator of climate-change-related events, it is also affected by other factors like crisis.

[Insert Figure 1 Here]

5 Pair-wise Climate Risk Spillover

In this section, we present the results of Granger causality in risk at $\tau = 5\%$ and 95% (the down-to-down and up-to-up scenarios). We present the results with the lag from one to ten weeks ($M = [1, 10]$). We first show the results using the data for the whole sample period. Then, since in

Figure 1 we find that the climate risk times also reflect non-climate-change-related events such as COVID-19 crisis, we provide a rolling window analysis, with a windows size of 150 weeks and a step size of four.

5.1 Climate Risk Spillover in the Whole Period

Table 2 presents the p-value of Granger causality test. Only $p < 10\%$ will be marked with color and a deeper color means a smaller value and thus a stronger causality relationship. We do observe climate risk spillovers among different markets. In Panel A, a large positive climate risk shock in Australia can transfer to the US, Japan and Europe one week after. Shocks in China can transmit to Japan and have lasting effects even after ten weeks. Panel B shows the Granger causality in risk at $\tau = 5\%$. Negative extreme shocks in the US have a significant predictive power for negative extreme shocks in the Europe, Japan and Australia two weeks later. And the effect could last for at multiple weeks (with significant results even when M equals eight or nine). The most segregated market is Japan: large positive climate risk shocks in Japan do not spillover to other markets, and negative shocks have short impact to Canada, Europe and China. The second most segregated market is Australia. In comparison, negative climate risk shocks in the US can spill over to all other markets, and have lasting effects to Japan, Australia and Europe.

It takes different periods for climate risks to spill over across different markets. For example, a positive climate risk shock in the US takes four weeks to transfer to China, and in the situation of China to the US, it takes only one week to for the climate risk to transmit across borders. This implies that investors in different markets absorb and update their beliefs with different speed. In most cases, the climate risk can spillover within five weeks.

The climate risk spillover is asymmetric. For example, Australia Granger causes the US at $\tau = 95\%$ but not at $\tau = 5\%$; in the meantime, the US Granger causes Australia at $\tau = 5\%$ but not at $\tau = 95\%$. This could be explained by that negative and positive shocks due to climate change events are generated under different economic situations/conditions, and thus have different channels of risk spillover across markets.

[Insert Table 2 Here]

5.2 Climate Risk Spillover across Time

Since in Table 2, most pairs of countries have climate risk spillover within five lags, we here present the rolling window results within $M = 5$. That is, for each pair in each window, we run Granger causality in risk test from $M = 1$ to $M = 5$ to get five p-values, and then we present the minimum p-value of the five tests. We provide in Figure 2 and Figure 3 the result of the test at $\tau = 95\%$ and $\tau = 5\%$ respectively. In Panel B of each figure, we see that the climate risk spillover among different markets are detected mainly in two periods: periods around the Paris Agreement (2015 – 2016) and periods after the COVID (2020). During both periods, the climate risk were high as

shown in Panel B of Figure 1. Accordingly, the risk spillover found in the whole sample analysis does not apply to all windows. For example, at $\tau = 95\%$, China and the US have risk spillover only during the Paris Agreement period but not the COVID period. In comparison, the risk spillover from US to Japan happens only during the COVID period.

Such complicated risk spillover relationship among different markets implies that the climate risk spillover is event-specific. Though global events like Paris Agreements and COVID crisis all generate positive shocks (as shown in Panel B of Figure 1), the channel of risk spillover can also be different. In addition, the climate risk spillover depends on the type of market, because given the same source of risk shock, the risk spillover is different among different pairs markets.

[Insert Figure 2 – 3 Here]

6 Measuring the Climate Risk Spillover

We have examined the pair-wise risk spillover relationship using the Granger causality in risk test for both positive and negative extreme shocks. A further question would be to which extent the climate risk can spillover within a global network. For this purpose, we present in this section the spillover index constructed using the network of six markets.

In the previous section, we show that it takes time for the climate risk to spillover across markets, and most pair of countries can have risk spillover within five lags. Therefore, in this section, we compare the risk spillover network from one lag to five lags ($M = [1, 5]$). To see how climate risk spillover change overtime, we also present the result under the rolling window approach, with window size of 150 weeks and a step size of four weeks.

6.1 Static Spillover

We present the estimation results in Table 3 – 4. It is worth discussing what our spillover index is really capturing before moving on. Mathematically speaking, the total directional spillover index (the "From"/"To" column in those panels) measures to which extent the observed local climate shock is contributed by historical foreign climate shocks; the total spillover index (the bottom-right element) is the average of the elements in the "From" column and it measures the average spillover level in the network. Elements in the "Net" are calculated as "To" minus "From", and are the "netted" risk spillover level after considering both how much shocks received and how much shocks gave.

Economically speaking, though there is no definite framework about the pathways of climate risk spillover in the literature, possible pathways of climate risk spillover can be summarized into five categorizes: Finance, People, Trade, Biophysical and Geopolitical (Benzie et al., 2019 and

Hildén et al., 2016).[10] Although we measure the climate risk spillover through financial markets, because the climate risk time series can capture both physical and transitional risk (though only partly), the spillover index is a comprehensive indicator that can measure the level of risk spillover through all the above five pathways. We give an example of climate risk transmission through the pathway of international trade: a severe drought in the US is expected to reduce the production of soybean by 40% in this year (climate risk in the US, direct losses), which is captured by the climate risk time series in the US as a large positive shock. Since US is one of the major soybean producer, the reduction of the production causes the price of soybean in the commodity market to go up by 30%. Because China is the main importer of soybean, food industry in China is expected to suffer huge increase in the production cost and then huge losses in the future. Such negative perspective is captured by investors in China and then a positive shock in the climate risk time series in China (Climate risk in the US transmitted to China). From the example, we can see that the climate risk transmission through international trade pathway can also be captured by the financial-market-based spillover index. In this example, the level of risk spillover is captured by cell (2,1) in each panel.

Table 3 shows the climate risk spillover at $\tau = 95\%$ (when there is a large positive shock). At a lag of three, Japan and Australia are the most segregated markets, with around 70% of the risk come from themselves. The situation for Australia changes a little at the lag of five, where there are large portion of risk spilled over from the US. This confirms the pair-wise results in Table 2. Europe is the main contributors of the risk spillover (with the highest value in the "To" row) at all lags. We provide in the last panel (the bottom-right panel) the average of the previous five panels. The main markets receiving the spillover are China and the US (with negative net spillover index). On average, around 30% – 40% of climate risk in each market is from outside (the "From" column).

Table 4 shows the climate risk spillover at $\tau = 5\%$, the extreme negative shock situation. The total level is higher than the 95% level: on average, around 40% – 45% of the climate risk in each market is transferred from outside (bottom-right panel, 'From' column). Compared to the 95% situation, Europe remains the largest net risk transmitter among all markets. the US changes from risk receiver to risk transmitter. The total level of climate risk spillover at $\tau = 5\%$ is also higher than at $\tau = 95\%$. One thing worth noting is that in both tables, as the lag M increase from one to three, the total spillover index (the bottom-right term, in bold term) increased drastically: at $\tau = 95\%$, the total spillover index increased from 16.97% to 38.64% and at $\tau = 5\%$, from 21.95% to 42.32%. After the lag of three, the speed of increase slows down. This implies that it takes around three weeks for the climate risk to be fairly transmitted.

[Insert Table 3 - 4 Here]

[10] Benzie et al. (2019) raised the first four pathways: the biophysical pathway can be cross-border ecosystems (e.g. floods or droughts upstream in a river basin); the trade pathway are consisted of international markets; the finance pathway means the flow of public and private capital; the people pathway means the movement of people across borders. Hildén et al. (2016) add the Geopolitical pathways, which means climate-related changes to international relations and strategies.

6.2 Dynamic Spillover

We provide in Figure 4 and 5 the net spillover, from- and to-spillover for each market, with window size of 150 weeks and a step size of four weeks. Considering the number of samples in each window (150) and based on the previous analysis, we set the lag to be three. Panel A of each table shows the total spillover index. We see that when there is major events (Paris Agreements) or crisis (COVID-19 crisis), the total level of spillover increased, at both $\tau = 5\%$ and $\tau = 95\%$. At the 5% situation, the level of spillover is higher in during the COVID crisis period. Panel B of both tables shows from- and to-spillover for each market. At both 5% and 95% situations, during periods around the Paris Agreement, the US, Canada and Europe are the main climate risk contributors. In the meantime, Japan, China and Australia are the main risk receivers. The role of risk transmitter/receiver can change over time. For example, during periods without global climate changes events (2017 – 2019), US is the net receiver and Europe is the net contributor. This could be explained by that during different periods, the source of climate risk shocks are different.

[Insert Figure 4 – 5 Here]

7 Determinants of Climate Risk Spillover

After studying how and to which extent the climate risk transmits among global markets, a further important question is what determines the climate risk spillover. Based on the discussion in Section 6.1, in this section, we study the relationship between our climate risk spillover measure and three types of pathways: Finance, Trade and Geopolitical.

7.1 The Model

We conduct the following time-series regression to explain the spillover among different markets (with robust error):

$$\begin{aligned} TS_t^\tau = \delta_0 + \delta_1 VIX_t + \delta_2 TS_t^{MKT} \\ \delta_3 r_t^{oil} + \delta_4 \triangle Export_t + \delta_5 GPR_t + \delta_6 \Delta EPU_t + \delta_7 CC_t + u_t \end{aligned}, \tag{7.1}$$

where TS_t^τ is the total spillover index (Eq. 2.13) under the rolling window at level τ, with $\tau = 5\%$ and 95%. The setting to calculate TS_t^τ is the same as the previous section, with window size of 150 weeks, a lag of three and step size of four. In total, we have 74 monthly observations of TS_t^τ. We choose six explanatory variables that represent the three pathways:

1. Finance Pathway:

- The equity market volatility index in the US (VIX_t^{US}) and Europe (VIX_t^{EUR}): The volatility index is the estimation of 30-day implied volatility of the S&P 500 index in the US (created by CBOE), and the 30-day implied volatility of the EURO STOXX 50 (created by Eurex). A high value of the volatility index means large overall uncertainty in the corresponding financial market. We choose the US and Europe because in previous section we show that the two markets are the main risk transmitters.
- The market connectedness (TS_t^{MKT}): TS_t^{MKT}measures to which extent different financial markets are connected to each other. To calculate TS_t^{MKT}, we first construct value-weighted market portfolios using all companies in the sample and then calculate the TS_t^{MKT} using the forecast error decomposition of Pesaran and Shin (1998).

2. Trade Pathway:

   - The oil price return (r_t^{oil}): The price comes from the West Texas Intermediate (WTI) crude oil price index. An increase of the oil price means that the economic activities are limited and possibly lower level of risk transmission.
   - World merchandise export volume indices ($\triangle Export_t$): the $Export_t$ measures the total export volume globally. We take the first difference to make it stationary. The data is from the World Trade Organization, with quarterly frequency. Since the regression is estimated at a monthly frequency, for $Export_t$, the monthly value is equal to the quarterly value it belongs to.[11]

3. Geopolitical Pathway:

   - The geopolitical risk index (GPR_t): The geopolitical risk index (GPR) is created by Caldara and Iacoviello (2022). It goes up when there is high geopolitical risk. High geopolitical risk could mean lower investment and employment and larger downside risks.

   - The change of Global Economic Policy Uncertainty (ΔEPU_t): The Economic Policy Uncertainty (EPU) is created by Davis (2016) to measure the policy and economic uncertainty. The index goes up during crisis periods (i.e. during crisis periods, $\Delta EPU_t > 0$).

Finally, we use the average of climate sentiment index of the six markets (CC_t). The climate sentiment index is the Google Trends index for the keyword of "climate change" and "global warming", and is calculated based on the amount of searches in a given period for a given region. The level of CC_t measures the total level of investor's attention towards climate change. A high global attention could mean that there could some world-wide climate change events and thus a possible high level of climate risk.

[11] https://stats.wto.org/

7.2 Results

We present in Table 5 the regression results for the whole period and in Table 6 the results before the COVID crisis. The coefficients of VIX US are negative under both $\tau = 5\%$ and 95%, which implies that high market uncertainty in the US lead to less climate risk spillover. The coefficient of the market connectedness (TS_t^{MKT}) is positive – this is to some degree reasonable because if financial markets are more connected, it would be easier for climate risk to transfer through the channel of financial markets.

The coefficient for the oil price r_t^{Oil} is insignificant in most cases. In comparison, the impact from the export is positive and significant during the pre-COVID period, which implies that a higher level of trading activities among countries will facilitate the spillover of climate risk. When we include the sample from the COVID, the coefficient becomes smaller and insignificant, which means that during the COVID period, trading may not be the main pathway for the climate risk transmission.

For the geopolitical risk index (GPR_t), the coefficient is significant and positive for $\tau = 95\%$ and is negative for $\tau = 5\%$, which implies higher uncertainly in the economic environment means higher levels of spillover for positive climate risk shock and lower levels of spillover for negative climate risk shock. During the COVID period, the size of coefficient becomes larger at both $\tau = 95\%$ and 5%. Similar observation applies to coefficients of Global Economic Policy Uncertainty (ΔEPU_t) (becoming more negative during the COVID period, though not significant), which means that the economic uncertainly plays a bigger role during the crisis period. Finally, the coefficient for the global climate sentiment is positive under both $\tau = 95\%$ and 5%, which implies that during periods when there are climate change events that have global impacts, the level of climate risk spillover is also higher.

[Insert Table 5 – 6 Here]

8 Conclusion

Climate change is a global phenomenon, which means that climate events in one place may transmit to other places due to the socioeconomic connection among countries in the world. If climate risk can transmit across borders, it will affect investors and companies who have high exposure to the climate risk. Since long-term climate risk is realized in the financial market as the arrival of climate news or changes in the climate sentiment, we study the climate risk spillover through financial markets. In concrete, we first construct a long-short portfolio using the return difference between low-emission companies and high-emission companies to capture the climate risk, and proxy the climate risk as the changes in the long-short portfolio. Then, we measure the climate risk spillover by studying the interaction of the proxy of climate risk among six markets: the

United States, China (including Hong Kong), Europe (including UK), Canada, Australia and Japan.

We provide international evidence that the climate risk is being priced in the six markets differently. The two markets with highest level of climate risk being priced are Australia and Canada. We observe similar trends of climate risk in different markets: when there are global-level climate events such as the signing of Paris Agreement or the outbreak of COVID, every market responds similarly.

We first study the pair-wise risk spillover among the six markets. We study two scenarios: when there are extreme positive climate risk shock and extreme negative climate risk shock. We evidence the climate risk spillover through the channel of financial markets and find that the climate risk spillover pattern among countries depends on the type of climate risk shock (positive or negative) as well as the market itself. In general, we find that Japan is the most segregated market, and the level of climate risk spillover is the highest around the event of Paris Agreement and the outbreak of COVID.

When we treat the six market as a whole in a network, we find that it takes around three weeks for climate risk to be fairly transferred. When there is a extreme positive shock in one market, around 30% will be transferred within five weeks. The level of transmission is higher for negative climate risk shock than for positive climate risk shock. Europe and the US are the main climate risk transmitters, and China and Japan are the main receivers of the climate risk. However, the role could change across time. For example, the US changed from net risk transmitters (during the Paris Agreement period) to net receivers (after the period). A plausible explanation is that during different periods, climate risk shocks can happen in different markets.

We then investigate the determinants of the climate risk spillover. In concrete, we examined three types of pathways that could possibly affect climate risk spillover: Finance, Trade and Geopolitical. When financial markets are more connected, climate risk can transfer more easily. A higher level of trading activities will facilitate the transmission of climate risk, especially during the pre-COVID period. The geopolitical uncertainty has increased impacts to the climate risk spillover during the COVID period. In addition, we show that the climate sentiment (measured by the Google Trends index) plays a role in affecting the climate risk spillover – higher climate sentiment means that the level of risk spillover is also higher.

In our paper, we study the climate risk spillover through linear models. However, it is possible that the climate risk spillover is non-linear, on which future studies could focus. That being said, our study still contribute to the literature by provide scholars with a method to capture the climate risk and to measure the climate risk spillover.

References

Amihud, Y., 2002. Illiquidity and Stock Returns: Cross-section and Time-series Effects. Journal of Financial Markets , 31–56.

Baker, M., Wurgler, J., 2006. Investor Sentiment and the Cross-Section of Stock Returns. The Journal of Finance 61, 1645–1680.

Benzie, M., Carter, T.R., Carlsen, H., Taylor, R., 2019. Cross-border Climate Change Impacts: Implications for the European Union. Regional Environmental Change , 763–776.

Berg, F., Koelbelz, J.F., Pavlova, A., Rigobon, R., 2021. ESG Confusion and Stock Returns: Tackling the Problem of Noise. Working Paper .

Bolton, P., Kacperczyk, M., 2022. Global Pricing of Carbon-Transition Risk. Working Paper .

Caldara, D., Iacoviello, M., 2022. Measuring Geopolitical Risk .

Carter, T.R., Benzie, M., Campiglio, E., Carlsen, H., Fronzek, S., Hildén, M., Reyer, C.P., West, C., 2021. A Conceptual Framework for Cross-border Impacts of Climate Change. Global Environmental Change 69, 102307.

Challinor, A.J., Adger, W.N., Benton, T.G., Conway, D., Joshi, M., Frame, D., 2018. Transmission of Climate Risks across Sectors and Borders. Philosophical Transactions of the Royal Society A: Mathematical, Physical and Engineering Sciences 376.

Chavleishviliy, S., Manganelli, S., 2021. Forecasting and Stress Testing with Quantile Vector Autoregression. Working Paper .

Chen, J., Liang, Z., Ding, Q., Liu, Z., 2022. Extreme Spillovers among Fossil Energy, Clean Energy, and Metals Markets: Evidence from a Quantile-based Analysis. Energy Economics 107, 105880.

Choi, D., Gao, Z., Jiang, W., 2020. Attention to Global Warming. The Review of Financial Studies 33, 1112–1145.

Davis, S.J., 2016. An Index of Global Economic Policy Uncertainty .

Diaz, D., Moore, F., 2017. Quantifying the Economic Risks of Climate Change. Nature Climate Change , 774–782.

Diebold, F.X., Yilmaz, K., 2014. On the Network Topology of Variance Decompositions: Measuring the Connectedness of Financial Firms. Journal of Econometrics .

Dong, X., Feng, S., Parida, S., Wang, Z., 2019. Corporate Social Responsibility Exposure and Performance of Mutual Funds. The Journal of Investing ESG Special Issue 28, 53–65.

Du, L., He, Y., 2015. Extreme Risk Spillovers between Crude Oil and Stock Markets. Energy Economics 51, 455–465.

Engle, R.F., Giglio, S., Kelly, B., Lee, H., 2020. Hedging Climate Change News. The Review of Financial Studies 33, 1184–1216.

Engle, R.F., Manganelli, S., 2004. CAViaR: Conditional Autoregressive Value at Risk by Regression Quantiles. Journal of Business and Economic Statistics 22, 367–381.

Fama, E.F., French, K.R., 1993. Common Risk Factors in the Returns on Stocks and Bonds. Journal of Financial Economics 33, 3–56.

Giglio, S., Kelly, B., Stroebel, J., 2021. Climate Finance. Annual Review of Financial Economics 13, 15–36.

Granger, C.W.J., 1969. Investigating Causal Relations by Econometric Models and Cross-spectral Methods. Econometrica 37, 424–438.

Han, H., Jung, W., Lee, J.H., 2019. Estimation and Inference of Quantile Impulse Response Functions by Local Projections: With Applications to VaR Dynamics. Working Paper .

Hildén, M., Groundstroem, F., Carter, T.R., Halonen, M., Perrels, A., Gregow, H., 2016. Ilmaston-muutoksen Heijastevaikutukset Suomeen (Cross-border Effects of Climate Change in Finland). resreport. Publications of the Government's analysis.

Hong, Y., Liu, Y., Wang, S., 2009. Granger Causality in Risk and Detection of Extreme Risk Spillover between Financial Markets. Journal of Econometrics 150, 271–287.

Koop, G., Pesaran, M.H., Potter, S.M., 1996. Impulse response analysis in nonlinear multivariate models. Journal of Econometrics 74, 119–147.

Lanne, M., Nyberg, H., 2016. Generalized Forecast Error Variance Decomposition for Linear and Nonlinear Multivariate Models. Oxford Bulletin of Economics and Statistics 78, 595–603.

Li, H.M., Wang, X.C., Zhao, X.F., Qi, Y., 2021. Understanding Systemic Risk Induced by Climate Change. Advances in Climate Change Research 12, 384–394. Including special topic on climate change and its impact on the ThirdPole and beyond.

Montes-Rojas, G., 2019. Multivariate Quantile Impulse Response Functions. Journal of Time Series Analysis 40, 739–752.

Pastor, L., Stambaugh, R.F., Taylor, L.A., 2021. Dissecting green returns. Working Paper .

Pesaran, H., Shin, Y., 1998. Generalized Impulse Response Analysis in Linear Multivariate Models. Economics Letters 58, 17–29.

PwC, 2013. International threats and opportunities of climate change for the UK. Technical Report.

Rehan, R., Nehdi, M., 2005. Carbon Dioxide Emissions and Climate Change: Policy Implications for the Cement Industry. Environmental Science and Policy 8, 105–114.

Santi, C., 2022. Investor Climate Sentiment and Financial Markets. Working Paper .

Su, X., 2020. Measuring Extreme Risk Spillovers across International Stock Markets: A Quantile Variance Decomposition Analysis. The North American Journal of Economics and Finance 51, 101098.

West, C.D., Stokeld, E., Campiglio, E., Croft, S., Detges, A., Duranovic, A., von Jagow, A., Łukasz Jarząbek, König, C., Knaepen, H., Magnuszewski, P., Monasterolo, I., Reyer, C.P., 2021. Europe's Cross-border Trade, Human Security and Financial Connections: A Climate Risk Perspective. Climate Risk Management 34, 100382.

White, H., Kim, T.H., Manganelli, S., 2015. VAR for VaR: Measuring Tail Dependence Using Multivariate Regression Quantiles. Journal of Econometrics 187, 169–188.

A Data Code

Table 7 presents the data code and data scope we use in Eikon's database.

[Insert Table 7 Here]

B Procedure to Construct the Long-short Portfolio

We construct the long-short portfolio under the two-sort strategies proposed by Fama and French (1993), with the following procedure:

- Company Selection: for every month m, companies that have enough carbon emission data from the last period (month $m-1$) will be included in the factor construction process. We also follow Amihud (2002) and the literature to exclude penny companies – companies whose price is below USD 5 at the time of formation in the US market. We check our sample of the US market and find that companies with a price below USD 5 take up around 5% of the total stocks. Therefore, since we are studying the global market, to align the standard across markets, we drop out companies with a price lower than the 5% quantile at the time of formation in each market.

- Independent Sort: we sort companies according to the month-end market value of month $m-1$. All are labeled into two groups: B(ig) and S(mall). The cut-off line is the median (50%) of all companies. Then, we sort again according to the CO2 emission. We set 30%/70% as the cut-off, and label the companies into three groups: H(igh) Emission, M(edium) E, L(ow) Emission. The result of the sort is a 2×3 label group.

– Portfolio Construction: We construct value-weighted portfolios within each label group, and get the long-short portfolio as

$$R_t^C = 0.5 \times (LB + LS) - 0.5 \times (HB + HS) \tag{B.1}$$

That is, we calculate the long-short portfolio as the return difference between low-emission companies and high-emission companies. For each month, we sort once and get a time series of one month. For example, at 2014/06, we sort and construct value-weighted portfolios using information from 2014/05. Then, the return of value-weighted portfolios from 2015/06 to 2016/05 will be used to construct the long-short portfolio.

C Using Simulation-based Method to Calculate the QIRF

In this section, we provide a discussion of how we use simulation-based method to calculate the QIRF. The process is similar to Koop et al. (1996) and Lanne and Nyberg (2016). The goal is to simulate the following quantile impulse response:

$$QGI_Y\left(H, \epsilon_{j,t}^*(\tau), \mathcal{F}_{t-1}\right) = Q\left(\tau, Y_{t+H} \mid \epsilon_{j,t}^*(\tau) = \epsilon_{j,t}(\tau) + \delta_j, \mathcal{F}_{t-1}\right) - Q\left(\tau, Y_{t+H} \mid \mathcal{F}_{t-1}\right).$$

In the above function, we aim to calculate the response of a variable specific shock. The shock size is δ_j, which is predetermined. The following process applies to calculate the response to a given shock δ_j:

1. Given the sample data, we estimate the model (2.9) and calculate the residuals $\hat{\epsilon}_t(\tau)$ (a matrix of $(K \times T)$).

2. We assume a constant covariance matrix for the residuals, and calculate the empirical covariance matrix $\hat{\Omega}(\tau)$ for $\hat{\epsilon}_t(\tau)$. We then convert the correlated residuals into uncorrelated by multiplying the inverse of a Cholesky factorization of the estimated covariance matrix: $\hat{\xi}_t(\tau) = P^{-1}\hat{\epsilon}_t(\tau)$, where $\hat{\Omega}(\tau) = PP'$.

3. Draw M times randomly from $\hat{\xi}_t(\tau)$ (in our case, we set M to be 1,000). For every draw m $(m = 1, 2, ..., M)$:

   (a) We get a matrix of $\xi^{(m)}(\tau) = (K \times (H+1))$ (i.e. for every draw m, we take $(H+1)$ vectors, with replacement, from the sample). Then, we recover the independent residual to dependent residuals: $\epsilon^{(m)}(\tau) = P\xi^{(m)}(\tau)$.

   (b) Based on the model (2.9), we use $\epsilon_t^{(m)}(\tau)$ and Y_{t-1} to calculate the realization of $Y_{t+H}^{(m)}(\mathcal{F}_{t-1})$.

   (c) Based on the model (2.9), we set $\epsilon_t^*(\tau) = \epsilon^{(m)}(\tau)_{(1)} + \begin{pmatrix} 0 \\ \delta_j \\ \dots \\ 0 \end{pmatrix}$, where $\epsilon^{(m)}(\tau)_{(1)}$ equals

to the first column of $\epsilon_t^{(m)}(\tau)$ and $\begin{pmatrix} 0 \\ \delta_j \\ ... \\ 0 \end{pmatrix}$ is a $(K \times 1)$ vector with only jth value to be non-zero. We then use $\epsilon_t^*(\tau)$, $\epsilon^{(m)}(\tau)_{(2:H+1)}$ and Y_{t-1} to calculate the realization of $Y_{t+H}^{(m)}\left(\epsilon_{j,t}^*(\tau) = \epsilon_{j,t}(\tau) + \delta_j, \mathcal{F}_{t-1}\right)$.

4. After getting the M realizations, we calculate the empirical quantile of the simulated $Y_{t+H}^{(m)}(\mathcal{F}_{t-1})$ and $Y_{t+H}^{(m)}(\epsilon_{j,t}^*(\tau), \mathcal{F}_{t-1})$

$$\begin{cases} \hat{Q}\left(\tau, Y_{t+H} \mid \epsilon_{j,t}^*(\tau) = \epsilon_{j,t}(\tau) + \delta_j, \mathcal{F}_{t-1}\right) = & q_\tau\left(\left\{Y_{t+H}^{(m)}(\epsilon_{j,t}^*(\tau) = \epsilon_{j,t}(\tau) + \delta_j, \mathcal{F}_{t-1})\right\}_{m=1}^{M}\right) \\ \hat{Q}\left(\tau, Y_{t+H} \mid \mathcal{F}_{t-1}\right) = & q_\tau\left(\left\{Y_{t+H}^{(m)}(\mathcal{F}_{t-1})\right\}_{m=1}^{M}\right) \end{cases} \tag{C.1}$$

5. Finally, the variable-specific impulse response is

$$Q\hat{G}I_Y\left(H, \epsilon_{j,t}^*(\tau), \mathcal{F}_{t-1}\right) = \hat{Q}\left(\tau, Y_{t+H} \mid \epsilon_{j,t}^*(\tau) = \epsilon_{j,t}(\tau) + \delta_j, \mathcal{F}_{t-1}\right) - \hat{Q}\left(\tau, Y_{t+H} \mid \mathcal{F}_{t-1}\right)$$

We apply the above process to each variable from $j = 1, ..., K$ to calculate the QIRFs. Then, the simulated $Q\hat{G}I_Y\left(H, \epsilon_{j,t}^*(\tau), \mathcal{F}_{t-1}\right)$ is put into Eq. (2.10), demonstrated as below, to calculate the QGFEVD:

$$\hat{\lambda}_{ij}(H) = \frac{\sum_{h=0}^{H-1}\left[Q\hat{G}I_Y\left(H, \epsilon_{j,t}^*(\tau), \mathcal{F}_{t-1}\right)_i\right]^2}{\sum_{h=0}^{H-1}\sum_{j=1}^{n}\left[Q\hat{G}I_Y\left(H, \epsilon_{j,t}^*(\tau), \mathcal{F}_{t-1}\right)_i\right]^2}.$$

We repeat the above process for N times and get the average of $\hat{\lambda}_{ij}(H)$ as our final QGFEVD.

C.1 Effectiveness of the Simulation Method

To test the effectiveness of our simulation method, we compare it with the analytical result of Pesaran and Shin (1998). For this purpose, we first generate two time series data from a preset two-variable VAR(1) model (with 443 observations):

$$\begin{cases} y_{1,t} = 0.5 + 0.5y_{1,t-1} - 0.2y_{2,t-1} + \varepsilon_{1,t} \\ y_{2,t} = 1 - 0.3y_{1,t-1} + 0.6y_{2,t-1} + \varepsilon_{2,t} \end{cases},$$

where $\varepsilon_{1,t}$ and $\varepsilon_{1,t}$ follows I.I.D normal distribution, with zero mean and a covariance matrix of $\Sigma = \begin{bmatrix} 0.4 & 0.01 \\ 0.01 & 0.4 \end{bmatrix}$. In the work of Pesaran and Shin (1998) the impulse response function is given by

$$\begin{aligned} GI_Y\left(H, \epsilon^*_{j,t}(\tau) = \delta_j, \mathcal{F}_{t-1}\right) &= E\left(Y_{t+H} \mid \epsilon^*_{j,t}(\tau), \mathcal{F}_{t-1}\right) - E\left(Y_{t+H} \mid \mathcal{F}_{t-1}\right) \\ &= A_H E\left(\epsilon_t \mid \epsilon^*_{j,t}(\tau)\right) = A_H \Sigma e_j \sigma_{jj}^{-1} \delta_j \end{aligned} ,$$

where A_H is the coefficient of the VAR model; e_j is a selection matrix; σ_{jj} is the jth diagonal item of the covariance matrix Σ; H is the forecast period. If we set $\delta_j = \sqrt{\sigma_{jj}}$, then the GIRF becomes

$$GI_Y\left(H, \epsilon^*_{j,t}(\tau) = \sqrt{\sigma_{jj}}, \mathcal{F}_{t-1}\right) = A_H \Sigma \sigma_{jj}^{-\frac{1}{2}} e_j \ , \tag{C.2}$$

which measures the effect of one standard error shock to the jth equation at time t on expected values of Y at time $t + H$.

If the simulation-based QIRF works well, then given the same size of shock (i.e., $\delta_j = \sqrt{\sigma_{jj}}$), the QIRF under $\tau = 50\%$ should have similar result as the analytical function of Eq. (C.2). Table 8 shows the GFEVD under Eq. (C.2) and the simulation-based QIRF. As can be seen, the results under the two methods are quite similar. The slight difference is because the coefficient estimated under the 50% quantile regression is slightly different from the coefficient of the OLS estimation.

[Insert Table 8 Here]

Figures

Figure 1: Graphs of Climate Risk Series ($CRisk_{i,t}$) in Each Market

Panel A: Weekly climate risk time series

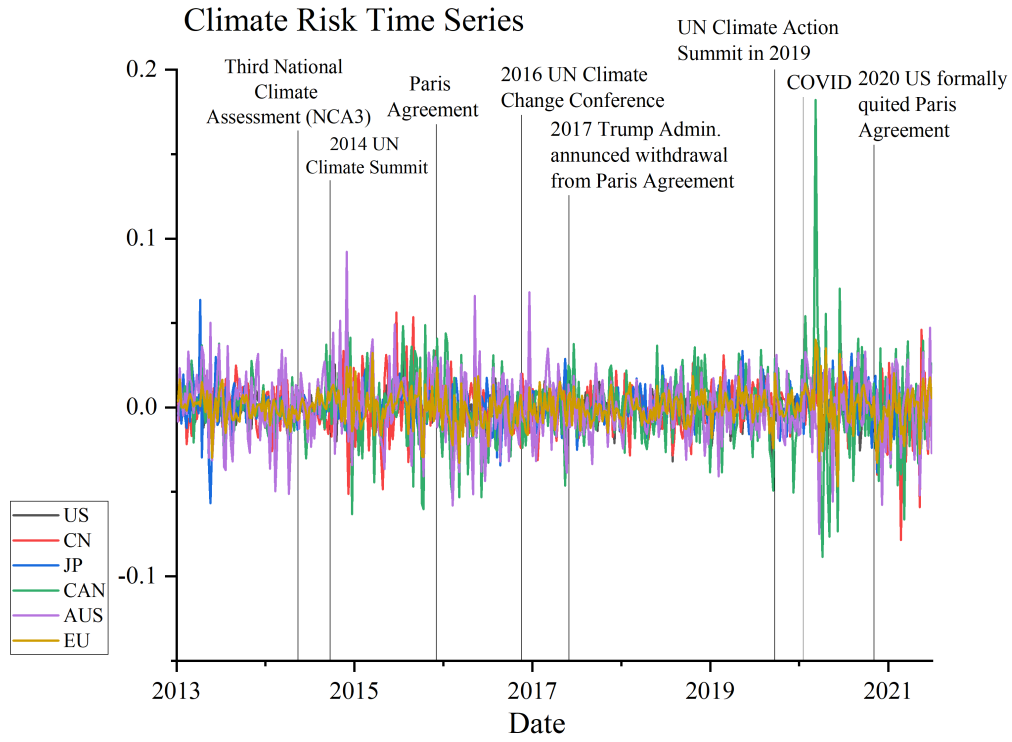

Panel B: Cumulative value of climate risk series

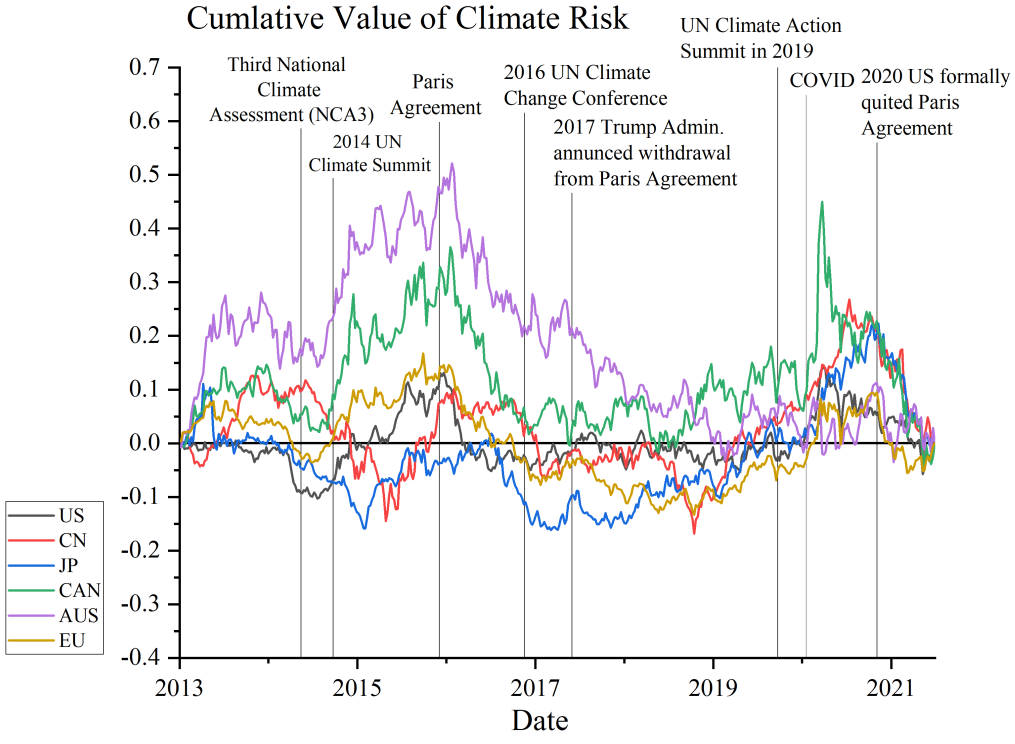

Note: Panel A shows the weekly time series of climate risk in each market. Panel B shows the cumulative value of climate risk time series for different markets, which is calculated as: $\sum_{t=1}^{T} CRisk_{i,t}$. In each graph, we plot major climate change events that happened during our sample period.

Figure 2: Granger Causality in Risk under Rolling Window at $\tau = 95\%$

Panel A: Granger Causality at $\tau = 95\%$ across time

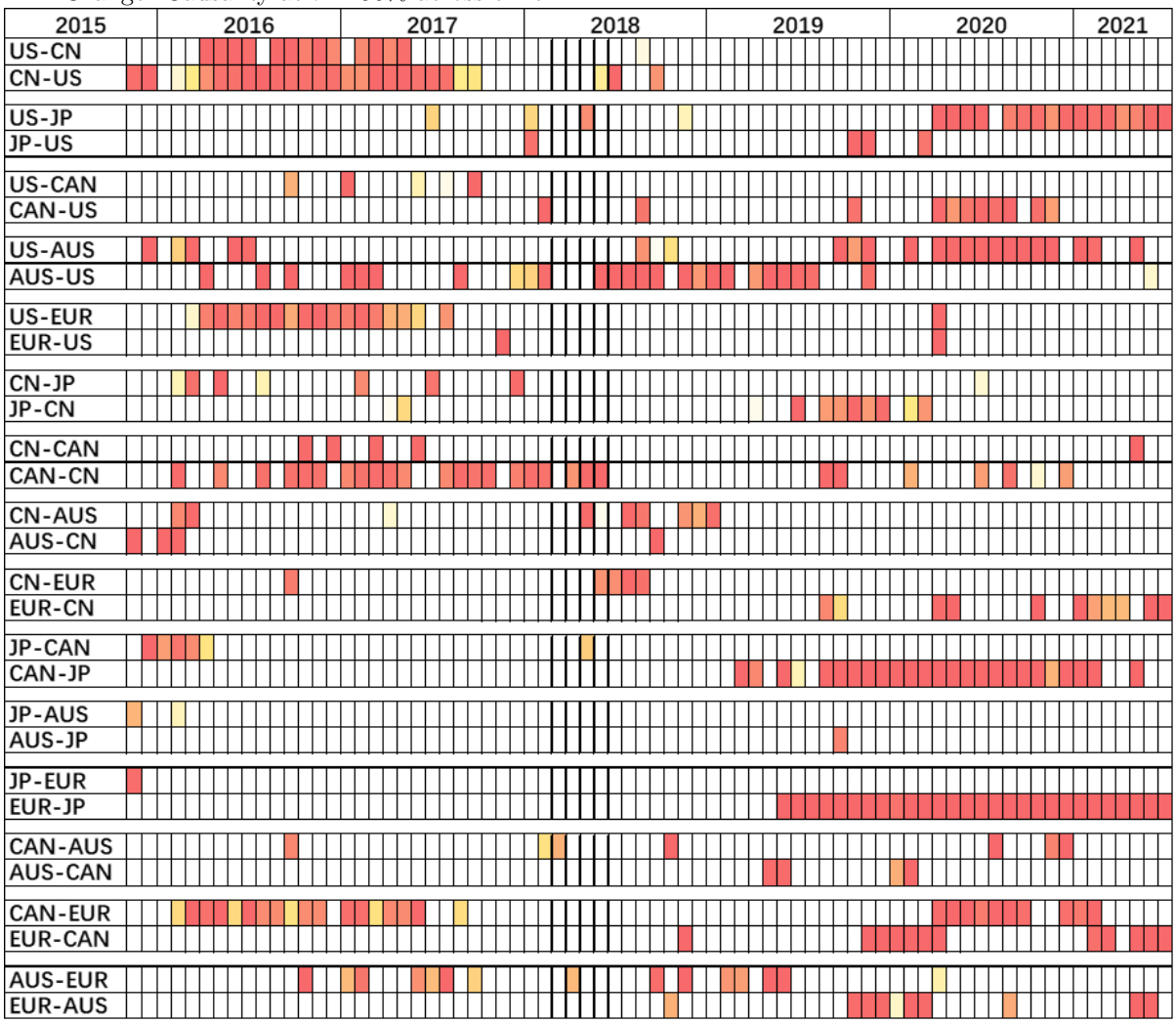

Panel B: Number of pairs with p-value smaller than 10%

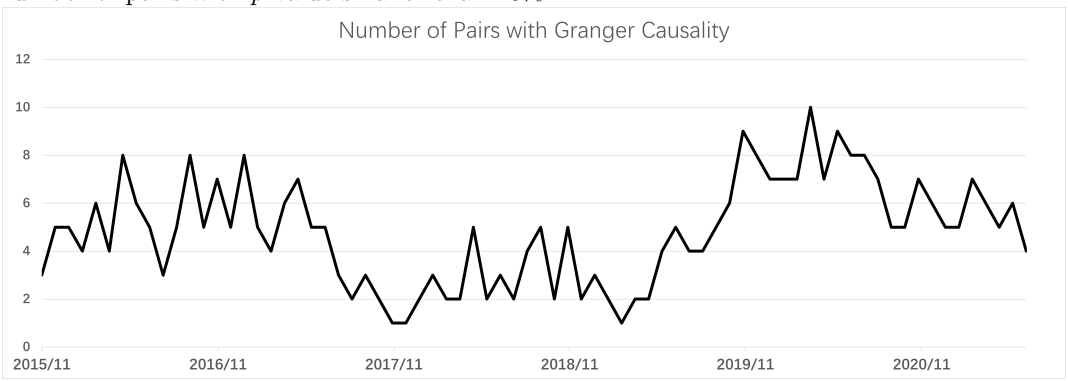

Note: The graph shows the p-value of Granger causality test at $\tau = 95\%$ under the rolling window method, with window size of 150 weeks and a step size of four weeks. For each pair in each window, we run Granger Causality in risk form $M = 1$ to $M = 5$ to get five test statistics, and then we present the minimum p-value of the five test statistics. "US-CN" means the test of if the US Granger-causes China; "CN-US" means the test of if China Granger-causes the US, and so on. Only $p < 10\%$ will be marked with color and $p < 10\%$ means there is Granger causality relationship. A deeper color means a smaller p-value. Panel B shows the number of pairs with significant Granger Causality test statistics in each window.

Figure 3: Granger Causality in Risk under Rolling Window at $\tau = 5\%$

Panel A: Granger Causality at $\tau = 5\%$ across time

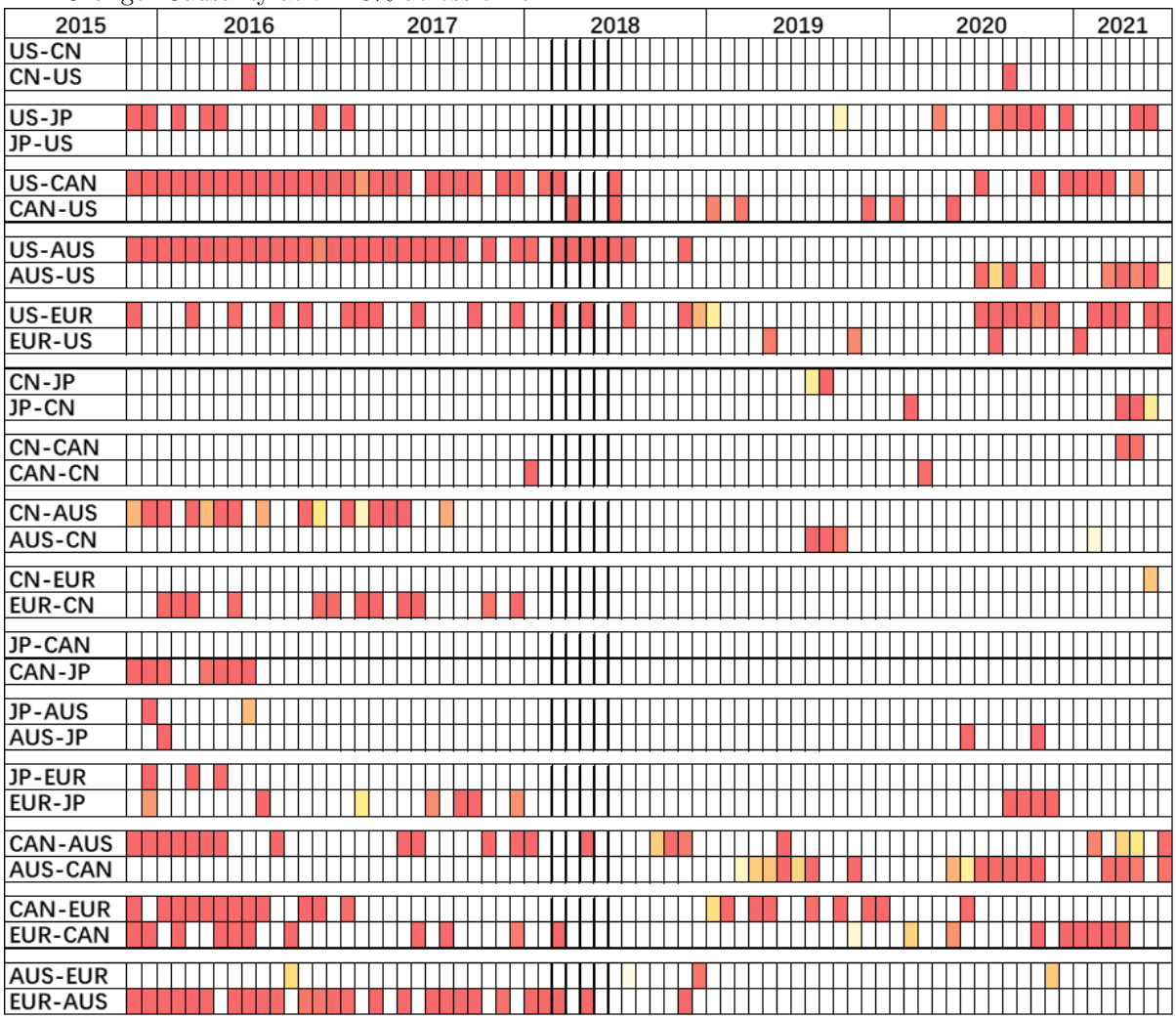

Panel B: Number of pairs with p-value smaller than 10%

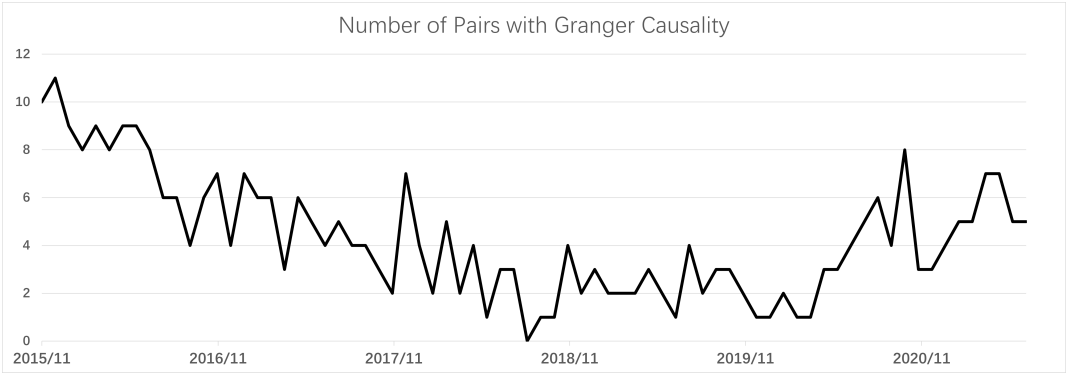

Note: The graph shows the p-value of Granger causality test at $\tau = 5\%$, with window size of 150 weeks and a step size of four weeks. For each pair in each window, we run Granger Causality in risk form $M = 1$ to $M = 5$ to get five test statistics, and then we present the minimum p-value of the five test statistics. "US-CN" means the test of if the US Granger-causes China; "CN-US" means the test of if China Granger-causes the US, and so on. Only $p < 10\%$ will be marked with color and $p < 10\%$ means there is Granger causality relationship. A deeper color means a smaller p-value. Panel B shows the number of pairs with significant Granger Causality test statistics in each window.

Figure 4: Dynamic Spillover at $\tau = 95\%$

Panel A: Total spillover over time

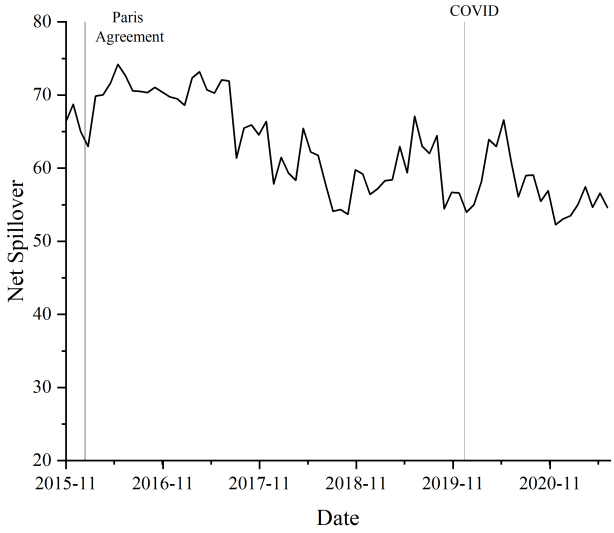

Panel B: Net spillover for each market

US	Europe	China
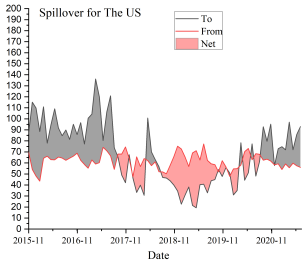	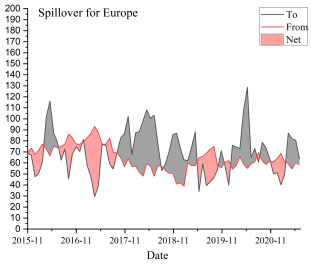	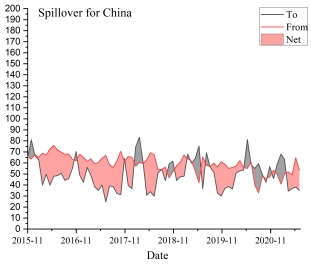
Australia	**Japan**	**Canada**
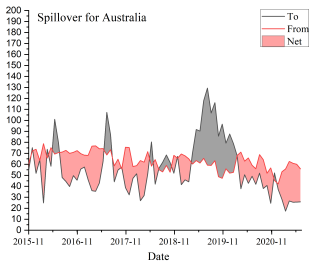	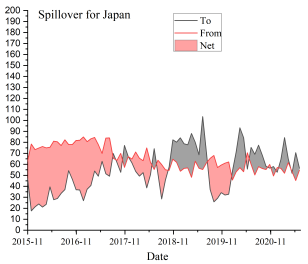	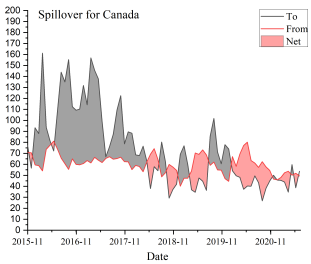

Note: The graph shows the dynamic spillover at $\tau = 95\%$ under rolling-window method, with window size of 150 weeks and a step size of one week (74 windows in total). Panel A shows the total spillover index of Eq. (2.13); Panel B shows the spillover index (Eq. 2.12) of each market. The red line is the total "From" and black like is "To". The distance between the two lines is the net spillover. We colored the area with red to denote a negative net spillover (From $>$ To, the net receiver) and gray to denote a positive net spillover (To $>$ From, the net giver). A positive value in the net spillover means the market is giving out impact and a negative value means the market is receiving impact from other markets.

Figure 5: Dynamic Spillover at $\tau = 5\%$

Panel A: Total spillover over time

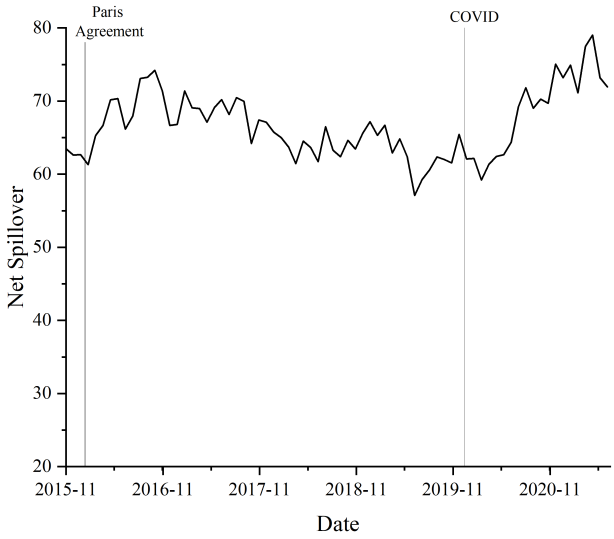

Panel B: Net spillover for each market

US	Europe	China
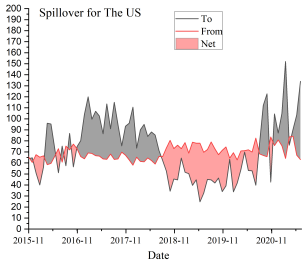	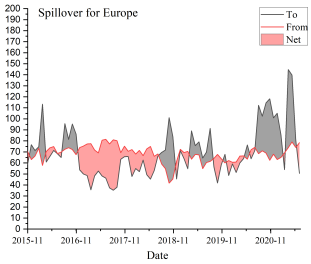	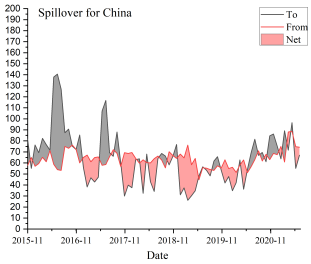
Australia	**Japan**	**Canada**
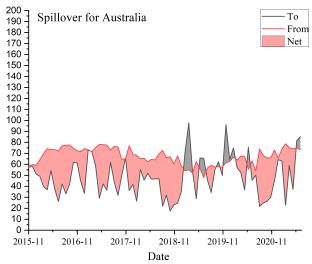	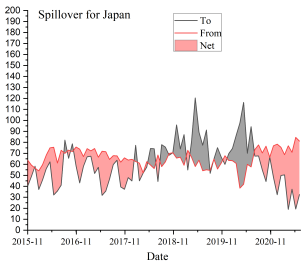	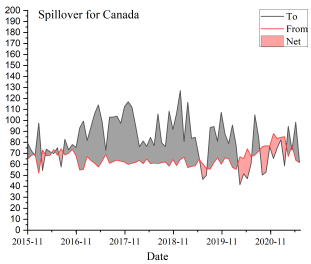

Note: The graph shows the dynamic spillover at $\tau = 95\%$ under rolling-window method, with window size of 150 weeks and a step size of four weeks. Panel A shows the total spillover index of Eq. (2.13); Panel B shows the spillover index (Eq. 2.12) of each market. The red line is the total "From" and black like is "To". The distance between the two lines is the net spillover. We colored the area with red to denote a negative net spillover (From > To, the net receiver) and gray to denote a positive net spillover (To > From, the net giver). A positive value in the net spillover means the market is giving out impact and a negative value means the market is receiving impact from other markets.

Tables

Table 1: Climate Risk Statistics for Each Market

Panel A: Climate risk statistics in each market

Factor stat.	**US**	**CN**	**JP**	**CAN**	**AUS**	**EU**
Mean	0.00%	0.00%	0.00%	0.00%	0.00%	0.00%
Std.	1.16%	1.46%	1.28%	2.37%	2.05%	1.06%
Max.	4.92%	5.64%	6.38%	18.21%	9.22%	4.02%
Min.	-5.44%	-7.86%	-5.69%	-8.86%	-7.51%	-4.68%

Panel B: Correlation among climate risk series of different markets

	US	**CN**	**JP**	**CAN**	**AUS**	**EU**
US	1					
CN	0.16	1				
JP	0.26	0.17	1			
CAN	**0.55**	0.10	0.23	1		
AUS	0.23	0.15	0.08	0.28	1	
EU	**0.59**	0.17	0.31	**0.59**	0.37	1

Note: Panel A shows the statistics of the climate risk time series in each market (from 2013/01/07 to 2021/06/28, 443 weekly obs.). Panel B shows the correlation among climate risk time series in different markets, all with 1% significance level.

Table 2: Granger Causality in Risk for Whole Period

Panel A: Granger causality in risk at 95% (the up-to-up situation)

M	US-CN	US-JP	US-CAN	US-AUS	US-EUR	CN-US	CN-JP	CN-CAN	CN-AUS	CN-EUR	JP-US	JP-CN	JP-CAN	JP-AUS	JP-EUR	CAN-US	CAN-CN	CAN-JP	CAN-AUS	CAN-EUR	AUS-US	AUS-CN	AUS-JP	AUS-CAN	AUS-EUR	EUR-US	EUR-CN	EUR-JP	EUR-CAN	EUR-AUS
1	0.75	0.95	1.00	0.97	0.95	0.14	0.02	0.89	0.79	0.17	0.79	0.43	0.72	0.98	0.85	0.00	0.08	0.18	0.12	0.12	0.00	0.14	0.05	0.93	0.00	0.71	1.00	0.44	0.98	0.84
2	0.55	0.74	0.73	0.46	0.73	0.75	0.05	0.54	0.06	0.61	0.55	0.78	0.76	0.58	0.54	0.68	0.77	0.05	0.43	0.78	0.00	0.79	0.34	0.42	0.39	0.63	0.78	0.60	0.58	0.33
3	0.36	0.59	0.74	0.76	0.57	0.58	0.02	0.10	0.04	0.55	0.65	0.77	0.58	0.56	0.63	0.77	0.62	0.03	0.77	0.81	0.00	0.83	0.77	0.48	0.45	0.62	0.59	0.12	0.61	0.34
4	0.22	0.39	0.82	0.47	0.04	0.41	0.00	0.06	0.10	0.68	0.65	0.85	0.78	0.69	0.69	0.73	0.38	0.09	0.44	0.81	0.00	0.77	0.48	0.35	0.48	0.59	0.45	0.16	0.69	0.81
5	0.03	0.39	0.84	0.50	0.01	0.24	0.01	0.61	0.11	0.63	0.66	0.82	0.36	0.61	0.58	0.53	0.27	0.14	0.46	0.85	0.00	0.81	0.54	0.47	0.53	0.62	0.00	0.01	0.77	0.39
6	0.01	0.23	0.72	0.79	0.00	0.24	0.01	0.23	0.00	0.52	0.61	0.83	0.18	0.55	0.62	0.53	0.33	0.16	0.33	0.87	0.00	0.80	0.38	0.71	0.49	0.65	0.44	0.00	0.78	0.68
7	0.00	0.41	0.65	0.85	0.01	0.28	0.61	0.31	0.23	0.57	0.56	0.88	0.36	0.19	0.55	0.47	0.46	0.15	0.68	0.85	0.00	0.83	0.35	0.71	0.68	0.72	0.45	0.02	0.78	0.30
8	0.01	0.35	0.70	0.63	0.15	0.19	0.01	0.40	0.37	0.53	0.57	0.81	0.28	0.14	0.59	0.44	0.39	0.20	0.52	0.83	0.00	0.80	0.72	0.36	0.36	0.75	0.41	0.03	0.79	0.58
9	0.00	0.00	0.64	0.66	0.01	0.19	0.06	0.66	0.79	0.58	0.62	0.88	0.20	0.63	0.42	0.42	0.25	0.09	0.47	0.84	0.00	0.76	0.28	0.35	0.32	0.78	0.42	0.04	0.73	0.11
10	0.00	0.33	0.66	0.78	0.01	0.33	0.08	0.49	0.80	0.41	0.63	0.76	0.82	0.13	0.60	0.44	0.39	0.30	0.21	0.80	0.00	0.51	0.24	0.34	0.20	0.81	0.41	0.02	0.74	0.09

Panel B: Granger causality in risk at 5% (the down-to-down situation)

M	US-CN	US-JP	US-CAN	US-AUS	US-EUR	CN-US	CN-JP	CN-CAN	CN-AUS	CN-EUR	JP-US	JP-CN	JP-CAN	JP-AUS	JP-EUR	CAN-US	CAN-CN	CAN-JP	CAN-AUS	CAN-EUR	AUS-US	AUS-CN	AUS-JP	AUS-CAN	AUS-EUR	EUR-US	EUR-CN	EUR-JP	EUR-CAN	EUR-AUS
1	0.99	1.00	0.92	1.00	0.88	0.00	0.81	0.47	0.99	0.37	0.46	0.60	0.83	0.83	0.24	0.31	0.47	0.13	0.79	0.01	0.22	0.06	0.73	0.56	0.05	0.99	0.95	0.44	0.98	0.60
2	0.50	0.00	0.77	0.00	0.00	0.76	0.73	0.77	0.77	0.43	0.73	0.58	0.02	0.47	0.05	0.55	0.45	0.78	0.05	0.51	0.36	0.55	0.78	0.78	0.58	0.47	0.00	0.02	0.77	0.02
3	0.57	0.00	0.50	0.00	0.05	0.46	0.77	0.59	0.12	0.43	0.60	0.62	0.13	0.77	0.60	0.82	0.82	0.81	0.02	0.44	0.62	0.74	0.72	0.78	0.46	0.54	0.07	0.08	0.61	0.47
4	0.04	0.00	0.57	0.00	0.00	0.56	0.78	0.42	0.09	0.56	0.74	0.60	0.11	0.49	0.71	0.58	0.59	0.75	0.00	0.01	0.70	0.74	0.71	0.79	0.79	0.65	0.49	0.06	0.74	0.69
5	0.07	0.00	0.72	0.00	0.00	0.66	0.84	0.35	0.00	0.52	0.70	0.64	0.39	0.49	0.68	0.13	0.64	0.76	0.04	0.06	0.60	0.25	0.73	0.87	0.86	0.00	0.77	0.31	0.84	0.69
6	0.66	0.00	0.72	0.00	0.00	0.64	0.77	0.32	0.00	0.52	0.65	0.77	0.20	0.21	0.21	0.83	0.87	0.90	0.05	0.58	0.40	0.69	0.65	0.75	0.80	0.00	0.42	0.62	0.34	0.72
7	0.66	0.00	0.69	0.00	0.00	0.52	0.75	0.23	0.01	0.49	0.65	0.77	0.25	0.66	0.59	0.64	0.69	0.89	0.00	0.04	0.50	0.67	0.68	0.80	0.73	0.76	0.80	0.70	0.67	0.14
8	0.46	0.00	0.76	0.00	0.00	0.61	0.65	0.43	0.00	0.59	0.62	0.01	0.29	0.27	0.17	0.83	0.80	0.89	0.04	0.49	0.81	0.02	0.58	0.80	0.90	0.26	0.76	0.83	0.23	0.70
9	0.63	0.00	0.00	0.00	0.00	0.66	0.75	0.38	0.03	0.62	0.56	0.38	0.61	0.61	0.78	0.67	0.88	0.91	0.10	0.51	0.59	0.65	0.40	0.84	0.83	0.00	0.07	0.51	0.06	0.26
10	0.44	0.00	0.78	0.00	0.12	0.55	0.76	0.47	0.12	0.47	0.61	0.60	0.45	0.27	0.65	0.72	0.75	0.92	0.18	0.30	0.56	0.65	0.82	0.78	0.78	0.83	0.57	0.50	0.80	0.31

Note: The table shows the p-value of the Granger Causality test. "US-CN" means the test of if the US Granger-causes China; "CN-US" means the test of if China Granger-causes the US, and so on. Only $p < 10\%$ will be marked with color and $p < 10\%$ means there is significant Granger causality relationship. A deeper color means a smaller p-value and thus a stronger causality relationship.

Table 3: Static Spillover among Different Markets ($\tau = 95\%$)

$M = 1$	US	CN	JP	CAN	AUS	EU	From
US	81.19	0.12	0.04	15.20	2.86	0.59	18.81
CN	0.23	76.55	0.12	6.88	0.51	15.72	23.45
JP	2.11	0.73	86.35	2.25	2.81	5.75	13.65
CAN	9.99	0.06	0.18	86.71	3.02	0.03	13.29
AUS	11.35	1.30	0.04	0.99	85.52	0.80	14.48
EU	3.13	1.77	0.49	11.87	0.89	81.84	18.16
To	26.81	3.97	0.88	37.19	10.09	22.88	**16.97**
Net	8.01	-19.48	-12.77	23.90	-4.39	4.72	

$M = 2$	US	CN	JP	CAN	AUS	EU	From
US	55.66	2.72	4.54	11.34	5.04	20.70	44.34
CN	1.11	76.46	2.84	8.34	0.86	10.39	23.54
JP	5.41	5.23	73.72	4.39	8.45	2.80	26.28
CAN	8.56	0.34	1.07	77.82	4.43	7.77	22.18
AUS	9.96	5.39	1.03	1.55	77.56	4.51	22.44
EU	0.99	1.05	3.00	9.84	11.49	73.63	26.37
To	26.03	14.73	12.49	35.46	30.27	46.16	**27.52**
Net	-18.31	-8.81	-13.79	13.28	7.83	19.79	

$M = 3$	US	CN	JP	CAN	AUS	EU	From
US	52.94	5.01	10.62	11.62	2.59	17.23	47.06
CN	5.47	58.36	4.69	10.61	4.52	16.35	41.64
JP	9.22	6.93	66.02	8.10	2.71	7.03	33.98
CAN	13.12	3.71	2.68	57.53	3.95	19.01	42.47
AUS	8.69	3.00	5.21	2.62	71.13	9.34	28.87
EU	11.75	1.65	7.60	12.28	4.54	62.18	37.82
To	48.25	20.31	30.79	45.23	18.31	68.97	**38.64**
Net	1.18	-21.34	-3.19	2.75	-10.56	31.14	

$M = 4$	US	CN	JP	CAN	AUS	EU	From
US	52.80	4.64	17.89	8.74	2.96	12.98	47.20
CN	5.03	62.65	3.41	7.10	8.30	13.51	37.35
JP	3.68	3.65	60.08	5.36	6.77	20.47	39.92
CAN	11.62	5.05	10.86	54.25	3.37	14.85	45.75
AUS	10.08	2.93	5.54	3.63	69.53	8.29	30.47
EU	3.14	3.85	11.34	12.78	5.70	63.19	36.81
To	33.54	20.13	49.03	37.62	27.09	70.09	**39.58**
Net	-13.66	-17.22	9.11	-8.13	-3.39	33.29	

$M = 5$	US	CN	JP	CAN	AUS	EU	From
US	41.64	7.92	17.45	9.37	5.05	18.57	58.36
CN	4.26	57.48	5.72	6.55	9.06	16.93	42.52
JP	4.68	5.88	61.84	9.53	4.24	13.83	38.16
CAN	5.89	4.26	12.39	63.88	6.42	7.16	36.12
AUS	18.29	3.97	7.90	8.75	54.47	6.62	45.53
EU	7.04	5.45	13.46	10.98	5.73	57.33	42.67
To	40.16	27.47	56.93	45.19	30.51	63.10	**43.89**
Net	-18.21	-15.05	18.77	9.07	-15.02	20.44	

Average	US	CN	JP	CAN	AUS	EU	From
US	56.85	4.08	10.11	11.25	3.70	14.01	43.15
CN	3.22	66.30	3.36	7.90	4.65	14.58	33.70
JP	5.02	4.48	69.60	5.93	4.99	9.97	30.40
CAN	9.83	2.69	5.44	68.04	4.24	9.76	31.96
AUS	11.67	3.32	3.95	3.51	71.64	5.91	28.36
EU	5.21	2.75	7.18	11.55	5.67	67.64	32.36
To	34.96	17.32	30.03	40.14	23.26	54.24	**33.32**
Net	-8.20	-16.38	-0.37	8.18	-5.10	21.88	

Note: The table shows the spillover network under $\tau = 95\%$. Each panel shows the network with a certain lag. The column named "From" shows total directional spillover from all other markets to market i, whereas the row named "To" shows total directional spillover to all other markets from market j. The row "Net" shows the total net pairwise directional spillover (to minus from). The bottom-right element (bold one) is the total spillover, which measures the total level of spillover of the net work. The last panel (bottom-right) is the average of the first five panels.

Table 4: Static Spillover among Different Markets ($\tau = 5\%$)

$M = 1$	**US**	**CN**	**JP**	**CAN**	**AUS**	**EU**	**From**
US	86.56	1.20	7.33	0.37	0.40	4.14	13.44
CN	1.85	75.46	13.97	1.33	1.51	5.88	24.54
JP	1.11	0.16	77.59	2.96	1.28	16.89	22.41
CAN	18.91	0.07	3.23	72.69	3.15	1.95	27.31
AUS	5.53	5.64	1.34	2.41	77.84	7.24	22.16
EU	8.46	0.06	2.96	5.23	5.13	78.15	21.85
To	35.87	7.13	28.84	12.30	11.46	36.11	**21.95**
Net	22.43	-17.41	6.43	-15.00	-10.69	14.25	

$M = 2$	**US**	**CN**	**JP**	**CAN**	**AUS**	**EU**	**From**
US	70.16	4.69	4.72	7.84	3.42	9.16	29.84
CN	28.43	53.85	2.03	13.23	0.22	2.25	46.15
JP	4.69	8.29	61.95	4.26	7.28	13.53	38.05
CAN	16.53	8.38	1.75	57.62	1.90	13.82	42.38
AUS	16.75	8.35	1.82	11.26	55.62	6.21	44.38
EU	15.82	6.03	1.25	2.46	6.55	67.88	32.12
To	82.22	35.75	11.58	39.04	19.37	44.97	**38.82**
Net	52.38	-10.40	-26.48	-3.34	-25.02	12.85	

$M = 3$	**US**	**CN**	**JP**	**CAN**	**AUS**	**EU**	**From**
US	57.20	11.89	11.29	7.45	2.78	9.39	42.80
CN	14.08	60.14	12.45	5.57	3.60	4.15	39.86
JP	7.35	7.23	60.92	1.86	5.36	17.28	39.08
CAN	9.25	14.08	9.14	55.88	2.77	8.87	44.12
AUS	9.36	9.06	4.54	8.98	51.70	16.36	48.30
EU	8.75	12.28	3.18	2.93	12.62	60.24	39.76
To	48.79	54.54	40.61	26.80	27.13	56.06	**42.32**
Net	5.99	14.68	1.53	-17.32	-21.17	16.30	

$M = 4$	**US**	**CN**	**JP**	**CAN**	**AUS**	**EU**	**From**
US	50.87	5.49	6.20	3.39	10.00	24.05	49.13
CN	18.47	52.81	9.32	7.65	6.20	5.54	47.19
JP	7.81	8.66	54.59	4.47	7.04	17.43	45.41
CAN	11.46	11.64	8.37	51.67	3.38	13.48	48.33
AUS	11.10	8.22	6.58	7.80	52.61	13.69	47.39
EU	17.03	8.26	5.12	2.40	15.01	52.16	47.84
To	65.88	42.26	35.60	25.72	41.64	74.20	**47.55**
Net	16.75	-4.93	-9.81	-22.61	-5.75	26.36	

$M = 5$	**US**	**CN**	**JP**	**CAN**	**AUS**	**EU**	**From**
US	36.71	5.27	12.50	13.86	6.28	25.39	63.29
CN	15.38	44.22	9.99	15.96	9.93	4.51	55.78
JP	8.09	7.55	57.24	10.47	5.16	11.50	42.76
CAN	10.56	13.40	14.58	42.46	5.55	13.46	57.54
AUS	16.07	12.55	3.75	4.50	51.37	11.77	48.63
EU	10.40	13.82	8.92	10.19	11.00	45.67	54.33
To	60.50	52.59	49.74	54.98	37.92	66.62	**53.72**
Net	-2.79	-3.19	6.97	-2.57	-10.71	12.29	

Average	**US**	**CN**	**JP**	**CAN**	**AUS**	**EU**	**From**
US	60.30	5.71	8.41	6.58	4.58	14.43	39.70
CN	15.65	57.29	9.55	8.75	4.29	4.47	42.71
JP	5.81	6.38	62.46	4.81	5.22	15.33	37.54
CAN	13.34	9.51	7.41	56.06	3.35	10.32	43.94
AUS	11.76	8.76	3.61	6.99	57.83	11.05	42.17
EU	12.09	8.09	4.29	4.64	10.06	60.82	39.18
To	58.65	38.45	33.27	31.77	27.50	55.59	**40.87**
Net	18.95	-4.25	-4.27	-12.17	-14.67	16.41	

Note: The table shows the spillover network under $\tau = 5\%$. Each panel shows the network with a certain lag. The column named "From" shows total directional spillover from all other markets to market i, whereas the row named "To" shows total directional spillover to all other markets from market j. The row "Net" shows the total net pairwise directional spillover (to minus from). The bottom-right element (bold one) is the total spillover, which measures the total level of spillover of the net work. The last panel (bottom-right) is the average of the first five panels.

Table 5: Regression Results for Spillover Index (Whole Period)

Dep. var. =	$TS_t^{95\%}$		$TS_t^{5\%}$	
	(1)	(2)	(3)	(4)
VIX_t^{EUR}	0.0215		-0.1587**	
	(0.19)		(-2.24)	
VIX_t^{US}		-0.2599*		-0.2237***
		(-1.89)		(-3.71)
TS_t^{MKT}	0.3343	1.1821**	1.8460***	2.0653***
	(0.63)	(2.31)	(4.17)	(4.65)
r_t^{Oil}	14.7369	6.2488	1.1995	-2.8383
	(1.91)	(0.63)	(0.24)	(-0.62)
$\triangle Export_t$	0.0396	-0.1117	0.2036***	0.1588**
	(0.40)	(-1.33)	(2.65)	(2.27)
GPR_t	0.1186***	0.0907***	-0.0160	-0.0315
	(3.30)	(2.60)	(-0.70)	(-1.44)
ΔEPU_t	0.0113	0.0189	-0.0272**	-0.0253**
	(0.40)	(0.71)	(-2.27)	(-2.07)
CC_t	0.2555***	0.2898***	0.1153**	0.0919**
	(3.45)	(4.73)	(2.15)	(1.99)
Constant	24.29	-20.53	-44.88	-55.38
Observations	74	74	74	74
Adjusted R-squared	0.21	0.27	0.46	0.52
VIF	1.49	1.49	1.49	1.49

Note: The table shows the time series regression results for model (7.1). In total, there are 74 weekly observations from 2015/11/16 to 2021/06/21. We report in the parenthesis the t-statistics. The "VIF" row is the average variance inflation factor of all explanatory variables and a VIF smaller than 10 means low level of multicollinearity. All explanatory variables are stationary under the Dick-Fuller test.

* Statistical significance at the 10% level.

** Statistical significance at the 5% level.

*** Statistical significance at the 1% level.

Table 6: Regression Results for Spillover Index (before COVID)

Dep. var. =	$TS_t^{95\%}$		$TS_t^{5\%}$	
	(1)	(2)	(3)	(4)
VIX_t^{EUR}	0.2953***		0.0524	
	(2.90)		(0.19)	
VIX_t^{US}		-0.2253		-0.2068*
		(-1.17)		(-1.89)
TS_t^{MKT}	1.5293*	1.5473**	0.9416	0.9054**
	(1.89)	(1.98)	(0.63)	(2.31)
r_t^{Oil}	24.7151*	15.9209	11.2543*	6.1804
	(1.78)	(0.94)	(1.91)	(0.63)
$\triangle Export_t$	2.0951***	1.8439***	0.8723	0.6913
	(6.02)	(4.65)	(0.40)	(-1.33)
GPR_t	0.0201	0.0287	-0.0201***	-0.0176***
	(0.82)	(1.17)	(3.30)	(2.60)
ΔEPU_t	0.0026	0.0056	-0.0094	-0.0078
	(0.09)	(0.21)	(0.40)	(0.71)
CC_t	0.1730***	0.2737***	0.0600***	0.0919***
	(2.95)	(4.81)	(3.45)	(4.73)
Constant	-41.8109	-37.3925	7.47287	12.8197
Observations	55	55	55	55
Adjusted R-squared	0.52	0.49	0.19	0.23
VIF	1.23	1.23	1.23	1.23

Note: The table shows the time series regression results for model (7.1), with samples before the COVID. In total, there are 74 observations from 2015/11/16 to 2021/06/28. We report in the parenthesis the t-statistics. The "VIF" row is the average variance inflation factor of all explanatory variables. All explanatory variables are stationary under the Dick-Fuller test.

* Statistical significance at the 10% level.

** Statistical significance at the 5% level.

*** Statistical significance at the 1% level.

Table 7: Data Description and Code

Name	**Frequency**	**Period**	**Code**
Price	Weekly	2013/01/07 - 2021/6/28	P
VIX^{EUR}	Weekly	2013/01/07 - 2021/6/28	.V2TX
Oil Price	Weekly	2013/01/07 - 2021/6/28	OILWTIN
Market Value	Monthly, month-end	2012/12/31 - 2021/6/30	MV
Total Emission	Monthly, month-end	2013/05/31 - 2020/12/31	ENERDP123

Table 8: IRFs under Two Methods

Panel A: The GIRF under Pesaran and Shin (1998)

H	$y_1 \to y_1$	$y_1 \to y_2$	$y_2 \to y_1$	$y_2 \to y_2$
1	99.37	0.63	0.63	99.37
2	97.22	2.78	6.53	93.47
3	94.51	5.49	12.38	87.62
4	92.52	7.48	16.22	83.78
5	91.20	8.80	18.59	81.41
6	90.34	9.66	20.07	79.93
7	89.79	10.21	21.00	79.00
8	89.43	10.57	21.60	78.40
9	89.18	10.82	21.99	78.01
10	89.03	10.97	22.25	77.75

Panel B: The simulation-based QIRF with $\tau = 50\%$

H	$y_1 \to y_1$	$y_1 \to y_2$	$y_2 \to y_1$	$y_2 \to y_2$
1	100.00	0.00	0.00	100.00
2	96.09	3.91	7.39	92.61
3	92.51	7.49	13.30	86.70
4	90.13	9.87	16.90	83.10
5	88.63	11.37	19.04	80.96
6	87.68	12.32	20.34	79.66
7	87.09	12.91	21.14	78.86
8	86.70	13.30	21.65	78.35
9	86.46	13.54	21.98	78.02
10	86.29	13.71	22.19	77.81

Note: The table shows the GFEVD with different types of IRFs and with the same size of shock $\delta_j = \sqrt{\sigma_{jj}}$. Panel A shows the results under Pesaran and Shin (1998) and panel B shows the QIRF with $\tau = 50\%$. $y_1 \to y_2$ means we give a shock to y_1 and see the response of y_2 in different periods.